



APPENDIX AVAILABLE ON THE HEI WEB SITE

Research Report 184

Advanced Collaborative Emissions Study (ACES): Lifetime Cancer and Non-Cancer Assessment in Rats Exposed to New-Technology Diesel Exhaust

Part 1. Assessment of Carcinogenicity and Biologic Responses in Rats after Lifetime Inhalation of New-Technology Diesel Exhaust in the ACES Bioassay

McDonald et al.

Appendix I. Characterization of Exposure Atmospheres in the ACES Bioassay

The HEI Exposure Characterization Review Panel reviewed the draft of this appendix and recommended revisions, which the investigator addressed in this revised version submitted shortly before the publication of Research Report 184. The panel was not able to review the revised version in time for publication. This appendix did not undergo the HEI scientific editing and production process but was proofread for spelling and grammar only.

Correspondence may be addressed to Dr. Jacob D. McDonald, Lovelace Respiratory Research Institute, 2425 Ridgcrest Dr., SE, Albuquerque, NM 87108; e-mail: JMcDonal@lrri.org.

Although this document was produced with partial funding by the United States Department of Energy (DOE), under the terms of Contract/Award Number DE-AC26-05NT42429, and certain motor vehicle and engine manufacturers, the opinion expressed herein are those of the authors and do not necessarily reflect the views of the DOE or motor vehicle and engine manufacturers.

© 2015 Health Effects Institute, 101 Federal Street, Suite 500, Boston, MA 02110-1817

**Health Effects Institute Advanced Collaborative
Emissions Study (ACES):
Characterization of Exposure Atmospheres in the
ACES Bioassay**

Jacob D. McDonald¹

Judith Chow²

Barbara Zielinska²

¹Lovelace Respiratory Research Institute
Albuquerque, NM

²Desert Research Institute
Reno, NV

CONTENTS

Abstract	3
Introduction	3
Specific Aims	4
Methods and Study Design	5
Engine and Exposure Facility	5
Atmosphere Characterization Methods	6
Sample Collection	7
PM Mass	7
Real-Time Mass and Size Distribution	7
Chemical Characteristics of PM	7
Gases and Vapors	9
Quality Assurance	10
Results	11
System Performance	11
Atmosphere Characterization	11
Gas Monitoring	12
PM	12
Chemical Composition of Atmosphere	13
Discussion	15
Conclusions	17
Implications of Findings	18
Acknowledgments	18
References	19
Additional Materials Available on the Web	20
About the Authors	20
Abbreviations and Other Terms	20
Tables	22
Figures	27

ABSTRACT

A characterization protocol was implemented to define rodent exposures during the Phase 3 chronic bioassay of the Advanced Collaborative Emissions Study (ACES) inhalation exposure study. The goal of Phase 3 of the ACES program was to evaluate the toxicity and carcinogenicity of new-technology diesel exhaust (NTDE) in Wistar Han rats. Previous HEI reports defined the system operations and characterizations conducted both during system commissioning and as part of the initial reports of the biologic response after 3 months (Mauderly and McDonald 2012; McDonald et al. 2012). Part 1 of the main report, to which this appendix is attached, includes the results of the lifetime study in rats. The goal of the exposures was to provide exposure atmospheres at a predetermined dilution defined by the concentrations of nitrogen dioxide (NO₂) in the test atmospheres. This was accomplished with exhaust generated from a 2007 Detroit Diesel Series 60 14.0-L on-highway certified heavy-duty diesel engine and its stock aftertreatment system. The engine was coupled to an alternating current dynamometer and operated on a repeating 4-hr engine cycle developed specifically for ACES. The exhaust was diluted with prefiltered air at targets of 4.2, 0.8, and 0.1 ppm NO₂. Test atmospheres were characterized in detail, with particulate mass, nitrogen oxides (NO_x), carbon monoxide (CO), and carbon dioxide (CO₂) being measured every day. Detailed assessments were conducted at four times throughout the studies: April 2010, September 2010, April 2011, and April 2012. An analyte list was prescribed that included approximately 200 analytes, including gases, semivolatile organic compounds (SVOCs), and metals, and detailed particle assessments. The major classes of gas-phase SVOCs that were measured included the straight chain and cyclic aliphatic acids and lower-molecular-weight polycyclic aromatic hydrocarbons (PAHs). Most of the volatile organic compounds (VOCs) were observed in the light (< C5) fraction, and most were acetylene and the alkanes/alkenes. Some aromatics were observed (e.g., toluene), but the benzene concentration was low.

This study included measurement of gases, particle mass, size distribution, real-time mass, and detailed chemical composition.

Over the course of the entire study, at an average of 4.4 ppm NO₂ in the high-exposure level, the nitrogen monoxide (NO) concentration was 6.6 ppm, CO₂ was 4794 ppm, CO was 6.4 ppm, and diesel-particle-derived particle mass concentrations were $\leq 12 \mu\text{g}/\text{m}^3$ on average. The ratio of NO:NO₂ changed throughout the study from approximately 1:1 at the beginning to approximately 2:1 toward the end, presumably because of expected degradation of the catalyst on the diesel particulate filter (DPF) that occurred with time. When measured in real time, the majority of the particle mass was observed during the one to two DPF regenerations that occurred during each 16-hr cycle. The particle number count also peaked during these periods and yielded particle size distributions that varied throughout the duty cycle, but were predominantly less than 50 nm in number diameter. The concentrations of these components, in general, scaled with dilution to the lower exposure levels. There were some exceptions to this scaling for some of the components that were revealed during the detailed characterizations of the test atmospheres. The detailed compositions of the test atmospheres are provided in the Additional Materials for this report.

For particle characterization, there was reasonable agreement (~15%) between weighed mass and the sum of measured species considering the uncertainty in each measurement. Depending on the atmosphere, carbon accounted for approximately one-third to one-half of the mass, and the carbon was primarily organic. The measurement of organic carbon (OC) was likely biased due to adsorption artifacts and contributions from the animals that made the organic measurements higher than actual. The inorganic ions (mostly sulfate and ammonium) composed about half of the mass as well. The remaining mass was made up of the elements. The composition of the test atmospheres, in general, showed only modest changes with time.

INTRODUCTION

The Health Effects Institute and its partners conceived and funded a program to characterize the emissions from heavy-duty diesel engines compliant with the 2007 and 2010 on-road emissions standards in the United States and to evaluate indicators of lung toxicity in rats and mice exposed

repeatedly to 2007-compliant, new-technology diesel exhaust (NTDE). The a priori hypothesis of ACES was that 2007-compliant, on-road diesel emissions "... will not cause an increase in tumor formation or substantial toxic effects in rats and mice at the highest concentration of exhaust that can be used . . . although some biological effects may occur." This hypothesis was tested at Lovelace Respiratory Research Institute (LRRI) by exposing rats through chronic inhalation as a carcinogenicity bioassay; measuring indicators of pulmonary toxicity in rats after 1, 3, 12, 24, and 28–30 months of exposure; and measuring similar indicators of pulmonary toxicity in mice after 1 and 3 months of exposure. A previous HEI report (Mauderly and McDonald 2012) describes the operation of the engine and exposure systems and the characteristics of the exposure atmospheres during system commissioning. Another earlier HEI report (McDonald et al. 2012) describes the exposure atmospheres and the biologic responses in mice and rats after subchronic exposure to NTDE. Part 1 of the current report (McDonald et al.) includes the results of inhalation exposure in near-lifetime exposure in rats. The motivation for this study was to evaluate the effects of NTDE in rats in the context of previous studies that had shown neoplastic lung lesions in rats exposed to traditional-technology diesel exhaust (TDE) (i.e., exhaust from diesel engines built before the 2007 U.S. requirements went into effect).

A 2007-compliant, 500-horsepower-class engine and aftertreatment system operated on a variable-duty cycle were used to generate the animal inhalation test atmospheres. Four groups were exposed to one of three concentrations (dilutions) of exhaust combined with crankcase emissions, or to clean air as a negative control. Dilutions of exhaust were set to yield average integrated concentrations of 4.2, 0.8, and 0.1 ppm NO₂. These dilution levels were selected based on the concentrations of NO₂ that were expected to yield a biologic effect at the high exposure level (attributed to NO₂) and no (NO₂-attributed) biologic effect at the lowest exposure level. Exposure atmospheres were analyzed by measurements of key components during each exposure day and by periodic detailed physical–chemical characterizations. Exposures were conducted 16 hr/day (overnight), 5 days/wk. Mice were exposed in initial studies up to 3 months as described earlier (McDonald et al. 2012). After the completion of the mouse exposure, rats were exposed and evaluated for up to 30 months. This report includes atmosphere-characterization information from both the mouse and the rat studies.

This report describes the results of the exposure-atmosphere characterizations that occurred during the Phase 3 chronic bioassay. It also includes a description of the engines and of the engine control and dilution systems, along with information on their performance. The objective of this report is to define what the animals were exposed to during the Phase 3B study, which will enable the exposure atmospheres and the results of the bioassay to be placed in the context of previous diesel studies with TDE and other NTDE studies that may be performed. Although much information could be garnered from detailed analysis of transient changes that occurred during the exposures on a particular day, the emphasis of this report is on describing the average concentrations in the emissions over the course of the study.

SPECIFIC AIMS

The overall aim of the research reported here was to characterize the composition of test atmospheres used for a chronic bioassay of 2007-compliant NTDE. The goal was to define exposure in detail as a means of ultimately interpreting the results of the bioassay and the stability of the test atmospheres over the duration of the study. The goal was *not* to define the durability of the engine–aftertreatment systems over a period of operation. Two engines and three aftertreatment systems were used over the course of the study because of swap-outs made necessary by required maintenance, repairs, or mechanical failure (for the emissions control system). *Neither* was the goal to compare the two different engine–aftertreatment systems that were used to generate the test atmospheres. The complexity of changing engines and aftertreatment systems at multiple times during the study and the impact of other factors, such as the presence of animals in the chamber, made it difficult to evaluate much more than the atmosphere composition over time. In order to avoid over-interpretation, the report stops short of trying to make these types of correlations. Specifically, the report provides the following: (1) descriptions of the engine and test facility and

atmosphere; (2) results of daily measurements and of control of exposure atmosphere concentrations/dilutions; and (3) description of the composition of test atmospheres during the course of the study and during four “detailed” measurement periods taken in April 2010 (during the mouse study), and September 2010, April 2011, and April 2012 (during the rat bioassay).

METHODS AND STUDY DESIGN

Engine and Exposure Facility

Two 2007 Series 60 14.0-L on-highway certified, heavy-duty diesel engines (termed B and B') and their stock exhaust gas recirculation (EGR) and aftertreatment systems (2007 compliant and diesel particle filter [DPF] model 6067HG6E) were used to generate test atmospheres for the ACES Phase 3B bioassay. Table 1 (at the end of this document) shows the engine use (measured in hours) throughout the study, the swap times of the engines and aftertreatment systems, and other key study milestones. At each oil change or in the event of an engine change-out, the engine was “mapped” as required by the 40 Code of Federal Regulations Part 86. Speed, torque, and power measurements were compared with the speed, torque, and power cycle demand values using the least squares method. All engine maps met the criteria for performance. Sample performance evaluations are included in Additional Materials I.A along with information on the engine/dilution system performance and exhaust chamber temperature. The representative data included in these Additional Materials are the data used to determine the primary and secondary dilution ratios (defined below), the engine performance, and the chamber temperatures during the detailed characterizations.

The system was mated to a Dyne Systems, 550-hp, 660-A, alternating current dynamometer and controlled remotely using a Dyne Systems, Inter-Loc V, Digital Multi-Loop Controller interfaced to a personal computer. The engine test cycle was controlled with the Dyne Systems Cell Assistant for Windows software. The engine was operated on a 16-hr duty cycle developed specifically for the ACES program (Clark et al. 2007). A local commercial source (Chevron-branded D-2 [legal for on-road use], Ever-Ready Oil Co., Albuquerque, NM) delivered diesel fuel meeting current on-road specifications to LRRI. The engine and associated systems were maintained as recommended by the engine manufacturer. Crankcase lubricating oil was changed every 250 hours. The oil was a proprietary blend approved by HEI and the Coordinating Research Council, provided by Lubrizol Corp., and also used in Phase 1 of the ACES program. The manufacturer-recommended oil filter was changed with each change of lubrication oil.

Exhaust was passed through a stock oxidation catalyst and particle aftertreatment system before injection into a 35.6-cm internal diameter dilution tunnel. The aftertreatment system was allowed to regenerate as needed during the operation of the engine. Figure 1 (at the end of this document) shows a diagram of the engine test cell and its coupling to the dilution tunnel. The crankcase ventilation effluent joined the exhaust stream downstream of the aftertreatment system. The exhaust was diluted with filtered air under turbulent conditions at the point of injection. The dilution tunnel supply-air flow was approximately 3000 cubic feet per minute. The primary dilution tunnel was a constant-pressure tunnel, rather than constant-volume. When exhaust flow increased, the increased pressure caused the dilution air to be dumped into a bypass leg in the test cell. At a distance of 5.5 m from the injection point (in the exposure room), a portion of the diluted exhaust was drawn through an in-line extraction probe. The exhaust mixture was withdrawn from the primary dilution plenum through individual probes and transit lines for each exposure chamber. This chamber and each exposure chamber had their own extraction probe and dilution system (Figure 2 at the end of this document). Subsequent to this extraction, the exhaust was diluted with filtered compressed air from a rotary dilution/dilution bypass system. Diluting flows were adjusted as needed to reach the final dilution and concentration targets. The residence time of DE in the dilution tunnel and transit lines was less than 5 seconds. After the exhaust reached the exposure chamber, the residence time was approximately 4 minutes. Exposures were conducted in 2-m³ exposure chambers (H1000/H2000, Lab Products, Elizabeth, New Jersey) that were specifically designed to enhance the homogeneity of material throughout the chamber. To accommodate the number of animals being studied, there were three chambers allocated per exposure group. The exposure data

presented are averages of each exposure group for each particular day or period. Prestudy evaluations of the test atmospheres in the chamber based on NO_x showed better than 10% homogeneity within the chamber (Mauderly and McDonald 2012). The chambers were operated on a push-pull system with house vacuum on the downstream side of the chamber and secondary dilution prior to the chamber. The system was balanced until the chamber pressure was slightly negative in pressure to ambient air. The flow through the chamber was monitored in real time to achieve the 4-minute residence time. Environmental conditions (i.e., temperature) were also monitored in real time. Environmental conditions are included in Additional Materials I.A.

All dilution and transit lines were constructed of stainless steel and were of nearly equal lengths for each exposure level. The primary dilution was calculated as the sum of the combustion air + tunnel flow + fuel consumption divided by the combustion air + fuel consumption. The secondary dilution rate was calculated based on the ratio of total NO_x measured in the primary dilution tunnel over the course of the engine cycle to that in the exposure chamber. The dilution ratio changed throughout the engine cycle due to differences in the load or work of the engine; the dilutions reported are the average over the cycle. The control chamber atmosphere consisted of filtered air. The dilution calculations and values during the detailed measurement campaigns are included in Additional Materials I.A.

Exposures were conducted 16 hr/day, 5 day/wk from approximately 1600 to 0800 hours Sunday through Thursday. Exposures were conducted for 16 hours plus the time to reach 90% of the target atmosphere (T₉₀). The system was operated without continuous operator presence between 1800 and 0800 hours, although surveillance personnel were always available and checked the system periodically during the night. Several control-alarm systems were in place to automatically shut down the engine and notify personnel in case of malfunction. The system was programmed to automatically terminate the engine cycle and switch the exposure chambers to clean dilution air at 0800 hours.

Atmosphere Characterization Methods

The measurements, sample conditions, and analytic techniques applied to chamber characterization are summarized in Table 2 (at the end of this document). Continuous concentrations of NO_x, made up of NO and NO₂, were measured daily at each exposure level throughout each exposure day. NO_x concentrations were also measured from the primary dilution tunnel to calculate the dilution ratio between the primary tunnel and the chambers. Continuous concentrations of CO, CO₂, and particle mass (using a Dekati Mass Monitor [DMM]), size distribution (using an aerodynamic particle sizer), and black carbon (using a photoacoustic spectrometer) were measured daily in the high-DE exposure chamber. Note that all real-time measurements were recorded once per second. Exposure atmosphere measurements were collected throughout the 16-hour exposure period. During periodic detailed characterizations, these measurements were taken at the other exposure levels, and on those days, the measurements were not made at the high-DE exposure level. Particle size was conducted once a week at each exposure level by the Fast Mobility Particle Sizer (FMPS; TSI, St. Paul, MN). A periodic measurement of size in the chamber was conducted with an Aerodynamic Particle Sizer (TSI). Particle mass concentration by gravimetric analysis of Teflon-membrane filters, at the inlet of the chamber and inside the exposure chamber, was measured once a week at each exposure level.

A more detailed characterization of particle mass and size was conducted once per week at each exposure level. Integrated particulate matter (PM) mass concentration was measured by gravimetric analysis of Teflon-membrane filters at both the inlet of the chamber and inside the exposure chamber. These two measurements allowed determination of how much PM the animals in the exposure chamber contributed to the total PM in the chamber. An FMPS was used to measure particle volume (mass), number, and number-based particle size distribution for particles between 5 and 500 nm in diameter, and an aerodynamic particle sizer was used to measure the mass-based size distribution.

Sample Collection

For the detailed characterization efforts — with the exception of the Teflon-membrane filter for metals, the filter/polyaromatic adsorbing resins (XAD)-4 cartridge for SVOCs (see below), and the cartridges for carbonyls — all chamber samples were collected from the breathing zone through sample ports. Samples were obtained through stainless-steel probes that were approximately 12 inches long and 0.25 inches in diameter.

PM Mass

PM mass concentration was measured gravimetrically by sampling for 16-hour intervals on 47-mm Teflon-membrane filters (TEFLO, Pall-Gelman, East Hills, NY) connected to the exposure chamber with a 0.6-cm internal-diameter probe connected to an aluminum in-line filter holder (In-Tox Products, Albuquerque, NM). PM mass concentration was also measured on filters (as described below) placed at the inlet to the exposure chamber just prior to entry or in the exposure chamber. This approach was taken because of the significant contribution of the animals to the PM concentration made within the chamber (including at smaller particle sizes). Prestudy characterizations showed that the chamber inlet was predictive of the contribution and composition of DE PM (DPM) present in the exposure chamber. Pre- and post-sample filter weights were measured using a Mettler MT5 microbalance. A static discharger was used prior to weighing filters to avoid any interference from electrical charge on the filters. The filters were not pre-conditioned to a specific temperature or humidity prior to or after collection.

Real-Time Mass and Size Distribution

Real-time PM mass was measured using a DMM-230 (Dekati, Finland) directly from the exposure chamber. The instrument was factory-calibrated and operated and maintained according to the manufacturer's recommendations. Particle size was measured by a combination of a fast-response differential mobility analyzer (approximately 5–500 nm) and an aerodynamic particle sizer (0.5–20 microns).

Chemical Characteristics of PM

Elemental and Organic Carbon Mass

Elemental carbon (EC) and OC masses were measured at the Desert Research Institute in PM samples collected on pre-baked quartz-fiber filters by the Interagency Monitoring of Protected Visual Environments (IMPROVE) temperature/oxygen cycle (IMPROVE TOR), as described by Chow and colleagues (1993, 2001).

A section of the filter sample was placed in the carbon analyzer oven such that the optical reflectance or transmittance of He-Ne laser light (632.8 nm) could be monitored during the analysis. The filter was first heated under oxygen-free helium purge gas. The volatilized or pyrolyzed carbonaceous gases were carried by the purge gas to the oxidizer catalyst where all carbon compounds were converted to CO₂, which was then reduced to methane quantified by a flame ionization detector (FID). The carbon that evolved during the oxygen-free heating stage is defined as OC. The sample was then heated in the presence of helium gas containing 2% oxygen. The carbon that evolved during this stage is defined as EC. Some organic compounds pyrolyzed when heated during the oxygen-free stage of the analysis and produced additional EC, which is defined as pyrolyzed carbon. The formation of pyrolyzed carbon was monitored during the analysis by the sample reflectance or transmittance. EC and OC were thus distinguished based on the refractory properties of EC using a thermal evolution carbon analyzer with optical (reflectance or transmittance) correction to compensate for the pyrolysis (charring) of OC. Carbon fractions in the IMPROVE method corresponded to temperature steps of 120°C (OC1), 250°C (OC2), 450°C (OC3), and 550°C (OC4) in a nonoxidizing helium atmosphere, and at 550°C (EC1), 700°C (EC2), and 850°C (EC3) in an oxidizing atmosphere.

OC Class and Species

SVOCs were collected using Teflon-impregnated, glass-fiber filters followed by XAD-4 resin cartridges. The target analytes included compounds that were statistically above detection limits during the Phase 1 component of the ACES program. Organic analyses for SVOCs were conducted at Desert Research Institute (Fujita et al. 2007).

Prior to extraction, the following deuterated internal standards were added to each filter and cartridge pair: naphthalene-d8, acenaphthylene-d8, phenanthrene-d10, anthracene-d10, chrysene-d12, pyrene-d10, benz[*a*]anthracene-d12, benzo[*a*]pyrene-d12, benzo[*e*]pyrene-d12, benzo[*k*]fluoranthene-d12, benzo[*g,h,i*]perylene-d12, coronene-d12, cholestane-d50, and tetrocosane-d50. Filters and XAD-4 were extracted with dichloromethane, followed by acetone, using the Dionex ASE. The extracts were then combined and concentrated by rotary evaporation at 20°C under gentle vacuum to approximately 1 mL and filtered through 0.45-mm Acrodiscs (Gelman Scientific). The extract was concentrated to 1 mL and split into two fractions.

The first fraction was precleaned by the solid-phase extraction technique (Wang et al. 1994a, b) using Superclean LC-SI SPE cartridges (Supelco) with sequential elution with hexane and hexane–benzene (1:1). The hexane fraction contained the nonpolar aliphatic hydrocarbons, hopanes, and steranes; the hexane–benzene fraction contained the PAHs. These two fractions were combined and concentrated to approximately 100 µL and analyzed by the gas chromatography–mass spectrometry (GC/MS) technique for hydrocarbons, hopanes, steranes, PAHs, and oxy-PAHs.

The second fraction was utilized for the polar compound analysis without precleaning. It was derivatized using a mixture of bis(trimethylsilyl)trifluoroacetamide and pyridine to convert the polar compounds into their trimethylsilyl derivatives. The second fraction was evaporated to 100 mL under moisture-filtered, ultra-high-purity nitrogen and transferred to 300-mL silanized glass inserts (National Scientific Company). Samples were further evaporated to 50 mL, and 25 mL of pyridine (Pierce), 25 mL of an internal standard mixture (succinic acid-d4, myristic acid-d27, and 1,2,4-butanetriol), and 150 mL of N,O-bis(trimethylsilyl)trifluoroacetamide with 1% trimethylchlorosilane (Pierce) were added. The glass insert containing the sample was put into a 2-mL vial and sealed. The sample was then placed into a custom-made thermal plate containing individual vial wells at 70°C for 3 hours. The calibration solutions were freshly prepared and derivatized just prior to the analysis of each sample set, and then all samples were analyzed by GC/MS within 18 hours to avoid degradation. Analysis of the polar organic compounds and the internal standards added has been described (Mazzoleni et al. 2007).

The extracts were analyzed for PAHs, alkanes, and polar compounds by GC/MS, using a Varian CP-3800 GC equipped with a CP8400 autosampler and interfaced to a Varian 4000 Ion Trap with electron impact (EI) ionization mode. The hopanes and steranes were analyzed using the Varian 1200 triple quadrupole GC/MS system with CP-8400 autosampler. Injections (1 µL) were made in the splitless mode onto a 30-m 5% phenylmethylsilicone fused-silica capillary column (DB-5 ms, J&W Scientific or equivalent). The individual compounds were quantified by selective ion storage technique, monitoring the molecular (or the most characteristic) ion of each compound of interest and the corresponding deuterated internal standard. Calibration curves for the GC/MS quantification were made for the most abundant and characteristic ion peaks of the compounds of interest using the deuterated species most closely matched in volatility and retention characteristics as internal standards. National Institute of Standards and Technology Standard Reference Material (SRM) 1647 (certified PAH) with the addition of deuterated internal standards and those compounds not present in the SRM (i.e., oxy-PAHs, nitro-PAHs, hopane, steranes, carpanes, hydrocarbons [HCs], and cycloalkanes) was used to make calibration solutions. A six- to eight-level calibration was performed for each compound of interest, and the calibration check (using median calibration standards) was run every 10 samples to determine the accuracy of analyses. If the relative accuracy of measurement (defined as a percentage difference from the standard value) was less than 20%, the instrument was recalibrated.

The nitro-PAHs were analyzed using the Varian 1200 triple quadrupole GC/MS system with CP-8400 autosampler. The tandem MS/MS system allows for structural elucidation of unknown compounds with precursor, product, and neutral loss scan. The GC interface allows for sensitive analyses of complex mixtures in EI as well as positive and negative chemical ionization (CI) mode. Negative CI offers a superior sensitivity for the analysis of nitro-PAHs (approximately 100 times higher than EI or positive CI) that could be emitted from combustion sources, including motor vehicle engines. The sensitivity of this instrument in full-scan EI/MS mode is approximately 1 pg/ μ L with 20:1 signal-to-noise ratio (S/N). In the EI/MS SIM mode, it reaches 50 fg/ μ L with 10:1 S/N. For negative CI, 10 fg/ μ L of octafluoronaphthalene gives an S/N of 20:1. This superior sensitivity offers the advantage of the ability to analyze small samples collected during a short sampling time.

Total Metals and Associated Elements

Samples for metal analysis were collected on clean Teflon-membrane filters and analyzed at the Desert Research Institute by energy-dispersive x-ray fluorescence (EDXRF) on a PANalytical Epsilon 5 EDXRF analyzer. Afterward, the Teflon-membrane filters were returned to their petri slides and stored under refrigeration until the EDXRF data were validated and indicated that the runs were acceptable.

Inorganic Ions: Ammonium (and Ammonia), Sulfate, Nitrate

One-half of the quartz filters (and blanks) that were collected for the carbon analysis were extracted and analyzed at the Desert Research Institute for water-soluble chloride, nitrite, nitrate, sulfate, and formic and acetic acid by ion chromatography. This extract was also analyzed for NH_4^+ by the indophenol colorimetric method.

Gases and Vapors

Oxides of Nitrogen, Total Hydrocarbons, Sulfur Dioxide, and Carbon Monoxide

NO_x were measured using chemiluminescent analysis (Teledyne Model 200 series; Ecophysics 700 series). CO and CO_2 concentrations were determined using a nondispersive infrared gas analyzer (California Analytical Model 600 series). Total hydrocarbons (THCs) were measured during the detailed characterizations using a real-time FID (Model 300H, California Analytical Instruments) calibrated against a certified propane standard. Sulfur dioxide (SO_2) was measured with a pulsed fluorescence analyzer (Thermo Electron Model 43i). Analyzers were zeroed daily using ultra-zero air and calibrated with National Institute of Standards and Technology–traceable span gases.

Gas-Phase Hydrocarbon Speciation

VOCs (except acids and carbonyls, which are too polar for collection and analysis from a canister) were collected using a custom-designed canister sampler (L. Sheetz Enterprises, Reno, NV). Samples were collected downstream of a NO_x denuder in a pre-cleaned Summa canister and analyzed within 30 days of collection to ensure accurate characterization of polar compounds that may “stick” to the canister walls. The NO_x denuder reduced NO_x that may react in the canister during storage with reactive analytes. Analysis was conducted at the Desert Research Institute by GC/MS.

Canister samples were analyzed for VOC species using GC/MS according to U.S. Environmental Protection Agency (EPA) Method TO-15. The GC-FID/MS system includes a Lotus Consulting Ultra-Trace Toxics sample preconcentration system built into a Varian 3800 GC with FID coupled to a Varian Saturn 2000 ion trap MS. The Lotus preconcentration system consisted of three traps. Mid-weight and heavier HCs were caught on the front trap consisting of 1/8-inch nickel tubing packed with multiple adsorbents. Trapping and eluting were performed at 55°C and 200°C, respectively. The rear traps consisted of an empty 0.040-inch inner-diameter nickel tubing for trapping light HCs and a cryo-focusing trap for mid-weight and heavier HCs isolated in the front trap. The cryo-focusing trap was built from 6-foot by 1/8-inch nickel tubing filled with glass beads.

Trapping on both rear traps occurred at -180°C , and elution occurred at 200°C . Light HCs were deposited into a Varian CP-Sil5 column ($15\text{ m} \times 0.32\text{ mm} \times 1\text{ }\mu\text{m}$) plumbed to a column-switching valve in the GC oven, then to a Chrompack $\text{Al}_2\text{O}_3/\text{KCl}$ column ($25\text{ m} \times 0.53\text{ mm} \times 10\text{ }\mu\text{m}$) leading to the FID for quantitation of light HCs. The mid-weight and heavier HCs cryo-focused in the rear trap were deposited into a J&W DB-1 column ($60\text{ m} \times 0.32\text{ mm} \times 1\text{ }\mu\text{m}$) connected to the ion trap MS. The GC initial temperature was 5°C , which was held for approximately 9.5 minutes, and then was increased at $3^{\circ}\text{C}/\text{min}$ to 200°C for a total run time of 80 minutes.

The system was calibrated with a mixture that contained commonly found HCs (75 compounds from ethane to *n*-undecane, purchased from Air Environmental) in the range of 0.2 to 10 ppbv. Three-point external calibrations were run prior to analysis, and one calibration check was run every 24 hours. If the response of an individual compound was more than 10% off, the system was recalibrated. Replicate analysis was conducted at least 24 hours after the initial analysis to allow re-equilibration of the compounds within the canister.

Analysis of Carbonyl Compounds

Carbonyl compounds were collected on dinitrophenylhydrazine (DNPH)-impregnated silica gel cartridges preceded by a commercially available oxidant scrubber and a Teflon-membrane filter to remove PM. To assess the trapping efficiency of the DNPH cartridge, two cartridges were used in series, and the backup cartridge was analyzed to ensure that all carbonyls were trapped on the first cartridge. Analysis was conducted at the Desert Research Institute by liquid chromatography/ultraviolet (UV) (photo-diode-array) detection. The hydrazones were separated and quantified per EPA Method TO-11A using a high-performance liquid chromatograph (HPLC; Waters 2690 Alliance HPLC System with 996 Photodiode Array Detector). After sampling, the cartridges were eluted with acetonitrile. An aliquot of the eluent was transferred into a 2-mL septum vial and injected with an autosampler into a Polaris C18-A $3\text{-}\mu\text{m}$ $100 \times 2.0\text{ mm}$ HPLC column. Since our HPLC system is equipped with the photodiode array detector, the identification of carbonyl compounds was much more accurate than with standard UV/visible detector. Using the photodiode array detector also enhanced the sensitivity of the analysis (Zielinska and Fujita 2003).

QUALITY ASSURANCE

This research was conducted in a manner that is consistent with many of the standards developed for Good Laboratory Practice, although full compliance was not a requirement of the protocol. Quality control (QC) consisted of the conduct of all work according to approved protocols and standard operation procedures, the inclusion of verified QC standards for the calibration of the certification of system performance, and third-party verification of all data before submission to the statistician for analysis. These QC processes applied to all aspects of the study, including the test and evaluation of engine performance, the verification of fuel and oil composition, and the analysis of test atmospheres. For each analytic tool, calibration or “span” checks were conducted during each time of use. The Quality Assurance Unit duties for the study protocol included evaluating study-start parameters, auditing exposure-system functions, auditing the processes of scientific data collection, and determining if data were recorded and stored as defined in the study protocol. The data were stored in a secure electronic database. Data in the report were derived using a wide range of methodologies for collection and analysis. Many of the analytes were collected in real time (i.e., gases, particle number), and some were integrated over time (i.e., filters). In cases where the data were collected in real time, they are shown in this report as either an average integrated for that exposure day (over the 16-hour exposure period) or an average of all of the measurements collected for the study. The error values associated with these measurements are the standard deviations when multiple measurements were made and detected for that analyte. When the values were measured only once at that level/time point and/or the levels were not detected, then the error shown in Table 3A (at the end of this document) is the root mean squared error of the square of the precision of the measurement \times concentration plus the detection limit. In the case of concentrations that go toward zero, the error becomes the detection limit. When the values were not detected for some analytes, they are listed as below the limit of detection (<LOD).

RESULTS

System Performance

As indicated above, Table 1 provides the engine use per month during the mouse and rat studies, distinguishing when each of the respective engines was used and noting milestones associated with the study or system maintenance and repairs. Prestudy testing put approximately 1200 hours of operation on each engine. During the study, engine B' was used from February 2010 through September 2011. That engine was replaced with engine B, which continued in operation until May 2012. Engine B' was installed in June 2012 and operated until the end of the study in December 2012. Engines were exchanged because of engine maintenance or repair requirements. At the end of the study, engine B' was used for 10,036 hours and engine B was used for 4015 hours.

Engine and dilution system performance are documented in Additional Materials I.A. This includes the average torque, power, exhaust temperature (pre- and post-DPF), dilution flow, combustion air flow, and fuel consumption. The data are summarized for each of the detailed measurement periods that were taken during the study. As shown, the engine conditions stayed reasonably consistent throughout the study, with noted changes in dilution air described below. Additional Materials I.A also includes select example engine "maps" that were performed each week as part of the engine/system check on performance. In this case a predefined steady-state engine cycle was performed to evaluate target versus actual performance for speed, torque, and power. The acceptance criterion for performance was 80% of target. The engine performed within the acceptance criterion throughout the study. The figures included in Additional Materials I.A for the engine maps show results typical of the performance that was observed.

There were some changes in the dilution flow and combustion air flow that had an impact on the primary dilution rate later in the study. Exhaust was diluted to achieve preselected target exposure concentrations of 4.2, 0.8, and 0.1 ppm NO₂. This required dilution ratios of approximately 25:1 to 30:1 at the high exposure level. The dilution rate in the primary dilution tunnel was approximately 5:1 in 2010 and 2011 (when engine B' was in use) and 12:1 in 2012 (when engine B was in use). Of interest is that the primary dilution ratio changed (to achieve the same NO_x levels) when the engines were swapped from B' to B.

Fuel and oil were analyzed at each change. Analytic data from the fuel and used oil analyses are included in Additional Materials I.D. Note that all fuel was within the specifications that the analytic labs follow (as noted in Additional Materials I.D) and that several of the oil analyses revealed increased (and sometimes excessive) levels of soot in the oil. The increased soot was likely a sign of the extremely tough conditions under which the engine was operated for the ACES cycle. The other major components of the used oil were phosphorous, calcium, zinc, and sodium.

Temperatures inside the exposure chambers at each exposure level during the detailed measurements periods are provided in Additional Materials I.A. Temperatures in the exposure chambers ranged from approximately 18 to 26°C. The presence of exhaust in the chamber increased the temperature within the chamber 1 to 3°C, with the highest temperatures generally associated with the highest exposure level.

Atmosphere Characterization

Table 3A (at the end of this document) provides the means of the major atmospheric components that were measured throughout the study (including the mouse exposure period). These means are study averages from the initiation of the study to the completion for each exposure level. Table 3B (at the end of this document) provides the means of the major components over the duration of the rat study only. Table 4 (at the end of this document) provides the summary composition of the high-exposure-level test atmospheres during each detailed characterization event in April 2010 (mouse study), and in September 2010, April 2011, and April 2012 (rat study). The detailed exposure-atmosphere compositions for the high level, as well as for the other exposure levels, for each detailed characterization are provided in Additional Materials I.B. The routine

monitoring data are provided in Additional Materials I.C. The composition of the test atmospheres, including commentary on the observed composition over time throughout the study based on the results of the four detailed characterizations, is described below.

Gas Monitoring

The following gases were routinely (daily) monitored: NO, NO₂, CO₂, CO, SO₂, and HCs. NO₂ concentrations, which were used as the dilution indicator, were within 10% of the target levels. The corresponding average concentrations of NO₂ were, over the course of the entire study, 4.4, 0.9, and 0.1 ppm, and those for NO were 6.6, 1.3, and 0.3. (For the course of the 30-month rat study, the averages were 4.2, 0.88, and 0.1 ppm NO₂, and 7.5, 1.7, and 0.4 ppm NO.) (See Tables 3A and 3B in this Appendix.) The concentrations presented are based on the integrated average over the 16-hour exposure cycle. As described below, the concentrations changed throughout the cycle. Of interest is that the NO:NO₂ ratio changed throughout the study. Table 4 presents the NO and NO₂ concentrations at the four different “detailed” characterizations. In April 2010, the NO:NO₂ ratio in NO_x in the high-exposure chamber was approximately 53:47 NO:NO₂ (engine B’). This ratio did not change significantly in September 2010 (engine B’). However, in April 2011 the ratio of NO:NO₂ was 62:38 (engine B’) and 67:33 in April 2012 (engine B). Due to the swap-out of the oxidative catalyst and DPF in September 2010 and the change of the engine, EGR, and DPF in September 2011, it is not easy to make comparisons regarding the function of the hardware with respect to the NO:NO₂ ratio. The outcome is an increase in NO from approximately 4.8 to 7.2 ppm from engine B’ over the period between April 2010 and April 2011. There was a corresponding increase of approximately 30% in CO₂ and NO_x (see Table 4) that reflected the difference in dilution over that time period. Also of note (see Additional Materials I.C) is that the tunnel NO:NO₂ ratios also showed a change over time, but the total NO_x levels present in the primary dilution tunnel did not while engine B’ was in use. This suggests that the change in NO_x in the chamber was due to the modification of the secondary dilution rate to accommodate the increase in the NO:NO₂ ratio. The change in NO_x in the primary dilution tunnel occurred later in the study, when engine B was installed and a higher primary dilution ratio was required. The concentration of CO was relatively low (< 10 ppm) and variable throughout the study.

Figures 3 and 4 (at the end of this document) indicate the real-time traces of the gases at each detailed monitoring period during one 16-hour ACES cycle. The plots show that, with the exception of THCs, all gases varied throughout the cycle as a function of duty cycle and DPF status. NO maximum concentration exceeded 20 ppm at some point during the cycle. NO₂ concentrations did not exceed 12 ppm at any point. During trap regeneration, the NO_x became almost completely NO because the conditions during that period did not favor conversion of NO to NO₂. CO₂ concentrations showed changes during the cycle that reflected primarily changes in fuel consumption. CO concentrations were the highest during the early part of the 16-hour cycle and decreased later, presumably due to improved conversion efficiency of the oxidation catalyst with increasing temperature during warm-up.

PM

Filter-based PM was also low in concentration, as expected. The composition of PM resulted from a combination of DPM and PM derived from animals in the chamber. The animal contribution undoubtedly included both dander and fine food dust. In addition, some PM likely formed in the chamber as a result of reactions between exhaust gases and ammonia, as previously shown (e.g., McDonald et al. 2004). Real-time particle mass and particle number/particle size distribution were also monitored routinely (daily), and representative illustrations of both are shown in Figures 5 and 6 (at the end of this document). The sample results were from the breathing zone of the rodents in the high-level exposure chamber during the detailed characterizations (September 2010 and April 2012 shown for number/size in Figure 6). Each plot represents measurements obtained during the 16-hour transient cycle. As indicated, particles were measurable primarily during two 90-minute regeneration periods. On most exposure days there were two trap regenerations. A minority of the days (i.e., 2–3 days/month) showed only one regeneration per cycle. The average particle mass

concentration during each 16-hour cycle did not increase significantly throughout the study. Any changes observed are likely within the measurement uncertainties of the assays. A typical average concentration of PM during a trap regeneration was approximately $50 \mu\text{g}/\text{m}^3$, with peaks ranging from approximately 70 to over $250 \mu\text{g}/\text{m}^3$. For the regeneration events shown, the particle number size distributions were both approximately 15–20 nm with a 1.5–2 nm geometric standard deviation. There were small changes in median number size that occurred over the duration of the study, but the changes were within 5 nm.

PM concentration was measured by both the filter and the DMM (see Table 3A). The filter PM mass concentrations were measured at the inlet to the chamber and in the chamber to allow the contribution from animals to be distinguished from the DE contribution. As expected, the concentration in the chamber (an average range of 17–27 $\mu\text{g}/\text{m}^3$ between clean air control and high-level atmosphere) was much higher than that in the chamber inlet ($< 8 \mu\text{g}/\text{m}^3$), showing that the major portion of PM mass was due to contributions from animals in the chamber. Of interest was that the difference between the measured filter PM in the high-exposure chamber and that in the control chamber was approximately equal to the concentration measured in the inlet in the high-exposure chamber. In other words, it is estimated that in the high-exposure level the PM consisted of approximately $8 \mu\text{g}/\text{m}^3$ diesel PM and 19–20 $\mu\text{g}/\text{m}^3$ background PM from the animals. As a result, filter particle mass concentration within the chambers was not closely dilution dependent. In contrast, the filter mass at the inlet was dilution dependent. Of further interest is that the PM concentration measured with the DMM in the chamber was consistent with the measured values of PM by filters at the inlet. The concentrations measured by the DMM “filter” out the dander measurements because it measures only submicron-sized particles.

The difference in particle number count was also dilution dependent, with the highest particle number observed in the high-level chamber. The particle number-based size distribution had a median size of approximately 20 nm, and the particle mass size distribution had a median size of 40 nm at the mid and high levels. This size and the transient nature of the particles associated with the trap regenerations were consistent with what was reported in Phase 1 of the ACES program (Khalek et al. 2011). The low and control levels had much larger particle sizes, but the mass concentrations were very low. Particle mass size distribution was measured with the FMPS (Table 3A) and an aerosol particle sizer (APS), which spans the larger size range of 0.5–20 microns. The APS detected very few particles (i.e., 1 particle/ cm^3) that did not change in character or amount between the control and high-exposure chamber. These few particles cannot be reliably measured by this technique, so the data are not presented, although we note that the particle size was approximately 3.5–4 microns with a geometric standard deviation of 2. Those particles are animal dander.

The PM concentration did not change appreciably over the course of the study. Any changes observed are likely within the measurement uncertainties of the assays. Particle counts in the exposure chambers were variable throughout the study and likely depended on the number of regenerations, the performance of the trap, and to a lesser extent the background. The particle count in the exposure chamber ranged from approximately 215,000 particles/ cm^3 in the low-exposure (average) level to 828,000 particles/ cm^3 at the high-exposure level on average. The concentrations fluctuated at different times throughout the study and reached a maximum of approximately 2 million particles/ cm^3 at one sampling. The overall high particle number count was similar to that reported for an earlier study that used 2000 diesel technology (McDonald et al. 2004). In that study, at a dilution of 10:1, the NO_2 concentration was approximately 5 ppm, and the particle count was approximately 1 million particles/ cm^3 .

Chemical Composition of Atmosphere

Figure 7 (at the end of this document) summarizes the composition of the atmospheres (at the rodent breathing zone) as the percentage of total measured mass for each chemical class. Figure 7 is a graphical representation of the summary data in Table 3A. As Figure 7 indicates, NO, NO_2 , and CO accounted for most of the mass of the measured components of the exposure atmospheres. The contribution of NO and NO_2 as a fraction of total mass increased proportionally with exposure

level, as expected. CO accounted for more proportional mass in the low level, mostly because of background CO relative to the low concentration of NO₂. In general, VOCs accounted for a small proportion of the mass, but because of the low concentrations of CO and NO_x, they accounted for up to 10% of the mass at the control and low-exposure levels. It is noteworthy that this result indicates that the animals contributed a significant portion of the measured VOCs. SO₂ was low at all exposure levels.

The total VOC concentrations generally did not trend precisely with dilution, but the highest concentration was observed at the high-exposure level. The concentrations at the lower exposure levels were not significantly higher than the control background. The VOCs that could be attributed to DE were primarily the alkanes (straight chain), alkenes, and aromatics. The VOCs listed by the EPA as mobile source air toxics that are of particular interest are benzene, toluene, ethyl benzene, and xylene (the four together are referred to as BTEX) and 1,3-butadiene. The concentrations of BTEX early in the study were very low and showed a trend toward increasing with DE-exposure level, especially benzene and toluene. In the 2012 measurement campaign (using engine B), the concentrations of the BTEX compounds were approximately five times higher than the earlier measurements using engine B'. For example, the concentration of benzene in April 2012 was 11.2 µg/m³ compared with approximately 2 µg/m³ in earlier measurements.

The carbonyls showed no concentration proportionality with dilution, and in fact were lower in concentration at the higher exposure levels. While animals do contribute to a background carbonyl concentration, the dilution-dependent decrease suggested that reactions occurred with NO_x at the time samples were being taken. Further investigation into the chromatograms (data not shown) from the carbonyl analysis suggested that, indeed, the NO_x-carbonyl reactions occurred at the high level. A cobalt oxide denuder was used in an attempt to remove NO_x before sampling; because the denuder was rapidly saturated, it was not effective.

PM composition was slightly different at each exposure level. This finding was shown by a change — an increase — in the proportional amount of inorganic PM. Changes in PM composition may be the result of reactions in the chamber between exhaust gases and ammonia produced by the rodents yielding nitrates/sulfates as previously described for animal inhalation studies with DE (McDonald et al. 2004). The proportions of OC relative to the total PM mass varied at different levels. Because the sum of OC and additional species exceeded the total measured mass, the OC measurements are considered biased by a sampling artifact (organic vapor adsorption). Furthermore, some of the OC measured in the chamber may have come from the animals, including dander and SVOC emissions from respiration. The high-exposure level had the largest contribution of PM that was derived from the engine. At that level, carbon accounted for about 50% of the mass, and the remainder was a combination of the inorganic ions and elements. The EC:OC ratio in Phase 3B for engine B was approximately 0.05 at the high-exposure level (measured during the April 2012 detailed characterization period), compared with 1.1 for engine B in Phase 1 (Khalek et al. 2009, 2011), suggesting a higher proportion of organic material in the particles collected in the chambers with the animals present. Figure 8 (at the end of this document) shows the measured EC and OC values from each sampling campaign. The OC concentrations were variable and higher than expected based on the likely actual concentration assumed from the determination of total PM, with excess concentration due to adsorption of vapor organics to the quartz filters during sampling. The OC was mostly found in the second fraction of the thermal analysis, suggesting it was primarily composed of compounds with moderate volatility. The EC concentrations also varied, but decreased over the course of the study (based on the three characterizations of engine B'), suggesting that the DPF efficiency improved over time with loading. In the last two measurement campaigns (conducted with engine B and B', respectively), the OC measurement artifact was substantially higher, resulting in an EC:OC ratio of approximately 0.05–0.1.

The elements were primarily zinc, manganese, copper, and iron. Potassium and calcium were also present. The metal concentrations were low and not substantially different from background in most cases. Figure 9 (at the end of this document) shows the total concentration of elements, as well

as iron, calcium, and zinc, during each detailed measurement campaign. As indicated, the total sum of measured elements did not change substantially (as a percentage of total atmosphere) over the course of the study (based on the three characterizations of engine B'), especially considering their relatively low levels. The values for calcium and zinc should mostly reflect fuel/lubricant additives. Their concentrations followed the general trend described above for total elements. Iron, which may reflect engine and component wear, showed a modest increase over the course of the study at the high-exposure level. At the lower levels, there appeared to be a decrease in iron concentration because of the high concentration measured in April 2010.

Among the measured SVOCs, the alkanes and polar compounds contributed the most to the test atmospheres, followed by PAHs. The polar compounds were primarily benzoic acid derivatives, and the alkanes were higher-molecular-weight compounds derived mostly from noncombusted fuel. Lower-molecular-weight compounds dominated the PAHs, primarily in the gas phase. Hopanes and steranes, as well as nitro-PAHs, were substantially lower in concentration than the PAHs, as expected. The hopanes and steranes indicated oil in the emissions. These compounds were increased slightly in the 2011 characterization relative to the two 2010 engine characterizations for engine B', suggesting that the aging of the system may have led to increased oil blow-by. There was no investigation of a potential change in oil viscosity, which may increase blow-by as well. Figure 10 (at the end of this document) shows the concentrations of these classes of compounds at each exposure level during each detailed measurement campaign. The hopanes and steranes, perhaps better than many of the measured atmospheric constituents, showed good dilutional linearity with changing exposure level (suggesting that the DE was the major contributor).

DISCUSSION

ACES Phase 3B was conducted to expose rats to three dilutions of NTDE derived from a 2007-compliant system. The test atmospheres were generated in an animal inhalation laboratory, and exposures were conducted in flow-through inhalation exposure chambers. Measurements from the chambers were conducted to characterize the nature of the test atmospheres in the presence of the emissions. In a previous report (Mauderly and McDonald 2012), the characterization of the system performance and of the chambers' atmospheres in the absence of animals was presented. In the current study, the focus was on the chamber atmospheres during a chronic rodent bioassay. The atmospheres are a dynamic mixture of diluted exhaust that vary throughout the transient engine cycle (including during regenerations) and are affected by the presence of the animals, including their excreta and exhaled breath, which contribute to the composition of the atmosphere directly and indirectly through chemical reactions. The atmosphere also varied because of changing engines and aftertreatment systems at points during the study, and because of some variance in dilution. Overall, the engine performance was good in terms of consistency of measured power, torque, and fuel consumption.

The test atmospheres reflected several key attributes that are characteristic of 2007-compliant engines and that distinguish NTDE from older (pre-2007) TDE. The concentrations of PM, SVOC, and VOCs were generally very low. This confirms the original expectations during the planning of ACES and the results in Phase 1 (Khalek et al. 2011). The most abundant pollutants were CO₂, CO, NO, and NO₂. Compared with earlier DE inhalation studies, the ratio of PM:NO₂ was at least three times lower. The NO:NO₂ ratio shifted over the course of the study possibly due to aging of the oxidation catalyst on the DPF. The result was less NO₂ in the exhaust. Because NO₂ was the primary dilution indicator and its level in the exhaust decreased over time for engine B, the degree of dilution had to be decreased over time. The dilution ratio was higher for engine B than for engine B'. This change in dilution for engine B' had only a modest impact on other atmosphere constituents because of the relatively variable emissions and low concentrations.

The overall composition of the test atmospheres revealed that animals contributed to the composition of the test atmosphere, both through dander and VOCs, but also because of reactions of these animal "emissions" with exhaust components. Measurements taken at the chamber inlet and compared with those from the chamber allowed the assessment of the differential amount of

PM from the animals and the engine exhaust. Data from the detailed characterization also showed that the animals contributed particle-bound organic compounds, which led to the formation of nitrate and sulfate particles and VOCs. The particle mass and number-based size distributions (determined with the FMPS, which measures particles up to only 500 nm) confirm the presence in the chamber of very small particles with a median diameter of 20 to 40 nm, which were considered to be derived almost exclusively from the engine.

Several prior major diesel studies set the stage for ACES. It is worth mentioning the major contrasts in the test atmospheres here benchmarked against those studies. It is also noted that the comparisons here are based on the test atmosphere composition and do not take into account in any detail of important variables such as differences in experimental configuration, dilution rates, engine size, or operating conditions. The focus is mainly on the composition and character of the test atmospheres and their qualitative differences. These previous studies were conducted with older technology, including a 1988 6.2-L light-duty diesel engine (Mauderly et al. 1994), a 1.6-L light-duty diesel engine (Heinrich et al. 1995), and a model 2000 5.9-L diesel engine (McDonald et al. 2004). The PM in the current study showed a very low to negligible contribution from EC, which is typically defined as soot. The atmosphere also contained low concentrations of VOCs and SVOCs, especially compared with previous studies of TDE (i.e., McDonald et al. 2004; Heinrich et al. 1995; Mauderly et al. 1994).

Exhaust from older technologies consisted of a high concentration of soot-laden PM, NO_x, CO, and HCs. The HCs and SVOCs contained high proportional concentrations (relative to 2007 technology) of aromatics and PAHs. In the exhaust characterization of a 2000 engine by McDonald and colleagues (2004), the EC:OC ratio was around 2.3 at the mid-exposure concentration versus 0.23 in the ACES Phase 3B study (with comparable NO₂ concentrations), indicating a much larger amount of soot from the older engine technology. NO_x for the older technology had a ratio of approximately 90:10 NO:NO₂ as compared with the current technology, where the ratio ranged from 50:50 to 70:30. The composition of the ACES test atmospheres revealed very low PM, SVOCs, VOCs, and CO, as expected. The PM concentrations at the highest exposure levels reported by Mauderly and colleagues (1994) in a study using a 1988 6.2-L engine were approximately 200 times higher than the ACES test atmosphere.

Despite significant decreases in many atmosphere components based on mass, the particle number was not much different in the current study compared with DE from model-year 2000 technology reported earlier (McDonald et al. 2004). This is important perhaps not because of the engine-out emissions (emissions that have not passed through a control or aftertreatment system) but in the interpretation of the animal exposure atmospheres. The differences in exhaust dilution (10:1 for the 2004 study by McDonald and colleagues, which was two to three times lower than the current study [25:1 to 30:1]) and other factors make it somewhat difficult to compare based on the emissions. Of note is also that the composition of the particles is quite different between the two technologies. The particle number concentration reported in that study was 1×10^6 particles/cm³ at the high-exposure level, which was conducted at a dilution of 10:1, a NO_x concentration of 45.3 ppm (NO₂ was 4.0 ppm), and a PM concentration of 1000 µg/m³. In the current study, the high-exposure level showed a particle number concentration of 0.8×10^6 particles/cm³ at a dilution of 25:1, PM of 7.8 µg/m³, and NO_x of 11.0 ppm (NO₂ = 4.4 ppm). The particle number concentration was transient in both studies, corresponding in the earlier study by McDonald and colleagues (2004) to changes in emissions during the engine test cycle and corresponding in the current study primarily to periods of DPF regeneration. As described elsewhere (Khalek et al. 2000, 2011; Swanson et al. 2009), the particles that contribute to the particle number from these two different technologies differ in composition, mostly related to the differences in their formation. In the 2007-technology diesel, the DPF regeneration corresponds to a significant increase in exhaust temperature, which leads to release of organic particles and sulfuric acid that serves as the nucleation source during dilution. As described by Khalek and colleagues (2011), the dilution conditions can lead to enhanced growth and formation of nanoparticles, and it is likely that

atmospheres in the animal exposure chambers had higher particle numbers because of the long residence time in the chambers (4 minutes).

The composition of the exhaust from the engine used in this study was characterized in Phase 1 of ACES and reported by Khalek and colleagues (2011). In that report, investigators reviewed the relevance of the emissions from the engine–aftertreatment system used here, benchmarked against several other competing technologies. They also compared the results to other reports on 2007-compliant emissions and placed the output in context. A comparison of the composition of the test atmospheres here to that broader literature is beyond the scope of the current report. However, it can be mentioned that the overall composition traits of the atmospheres reflected the composition reported by Khalek and colleagues (2011). They reported increased NO₂, low CO and HCs, and low PM relative to pre-2007 engines. The PM composition in that report (average of four technologies) was 53% sulfate, 30% OC, 13% EC, and 4% metals. In the current study, benchmarked against total measured PM, we show similar percentages of EC (~15%) and a lower direct contribution to sulfate. However, the total inorganic ions, which included nitrate, sulfate, and ammonium, accounted for about 50% of the mass at the high-exposure level. The higher percentage in the current study was due to the reaction of ammonia with the gases to convert nitric acid to ammonium nitrate. Of interest was that Khalek and colleagues (2011) did not detect nitrate in the Phase 1 characterization of this engine, affirming that the presence of the nitrate is due to the reaction with ammonia (from the animals) to form ammonium nitrate salts.

The contribution from the elements was slightly higher (compared with the Phase 1 work) in the current studies, at about 10% of PM. The majority of this mass was sodium, however, similar to the current study. The other elements were primarily calcium, zinc, and phosphorus (matching the composition of the lubrication oil). Regarding the speciated organics, Khalek and colleagues (2011) showed similar trends of high proportions of alkanes, single-ring aromatics, and lower-molecular-weight PAHs as the dominant measured organics (based on concentration), with low levels of the hopanes/steranes and nitro-PAHs. They also reported high concentrations of carbonyls, which were likely present in the current study, although measurements at the high level do not show this, probably because of inaccuracy due to sampling problems.

Overall, the test atmospheres in the current study were so low for many analytes observed in the previous reports that they were difficult to measure against the background measured in the chamber. Only NO_x, particle number, and CO were present at a similar magnitude of concentration to the components tested in the previous studies with older-technology engines. The overall composition of the test atmospheres in this study was different from prior studies of TDE both in terms of quantity and type of components present. The current study showed substantial decreases in soot and both volatile and nonvolatile organics, most notably.

CONCLUSIONS

DE from a 2007-compliant, heavy-duty diesel engine equipped with emission controls and selected from four candidate engines in Phase 1 of the ACES program (see Khalek et al. 2009, 2011) was used to generate test atmospheres for a chronic rodent bioassay. The engine was operated on a dynamometer and fueled with ultra-low-sulfur diesel fuel that met current on-road specifications. The engine and associated systems were maintained as recommended by the engine manufacturer. The crankcase lubricating oil, which was changed every 250 hours, was a proprietary blend provided by Lubrizol that had also been used in Phase 1 of the ACES program. The engine was operated on a 16-hour cycle that was specifically designed for ACES to represent a combination of highway and urban driving conditions.

The concentrations of PM, SVOCs, and VOCs were generally very low. This confirms the original expectations during the planning of ACES and the results in Phase 1 (Khalek et al. 2011). The most abundant pollutants were CO₂, CO, NO, and NO₂. In comparison to earlier TDE inhalation studies (Heinrich et al. 1995; Mauderly et al. 1994), the ratio of PM to NO₂ was at least 300 times lower. The NO:NO₂ ratio for engine B shifted over the course of the study, possibly due to aging of the oxidation catalyst on the DPF. The result was less NO₂ in the exhaust. Because NO₂

was the primary dilution indicator, the degree of dilution decreased over time. This change in exhaust dilution had only a modest impact on other atmosphere constituents because of the relatively variable emissions and low concentrations.

The overall composition of the test atmospheres revealed that animals contributed to the composition of the test atmosphere, both through dander and VOCs, but also because of reactions between these animal “emissions” and exhaust components. Data from the detailed characterization also showed that the animals contributed particle-bound organic compounds, which led to the formation of nitrate and sulfate particles and VOCs. The particle mass and number-based size distributions (determined with the FMPS, which measures particles up to only 500 nm) confirm the presence in the chamber of very small particles with a median diameter of 20 to 40 nm, which were considered to be derived almost exclusively from the engine. The PM in the current study showed a very low to negligible contribution from EC, which is typically defined as soot. The atmosphere also contained low concentrations of VOCs and SVOCs, especially compared with previous studies of TDE. The composition of the SVOCs showed relatively low and varying concentrations of PAHs. The metal concentrations were small and not substantially different from background in most cases.

IMPLICATIONS OF FINDINGS

The ACES Phase 3B investigations are the first of their kind to examine biologic responses in animals exposed to exhaust from 2007-compliant diesel technology. The results reported here define the test atmospheres from ACES. As expected, the atmospheres showed marked contrasts to those in earlier studies of pre-2007 diesel technology. The most notable differences were the significant decreases in the total VOCs, SVOCs, and PM measured in the exposure atmospheres. In addition to having lower component concentrations than are found in studies of TDE (i.e., year 2000 technology by McDonald et al. 2004; 1980 technology by Mauderly et al. 1994), the exhaust had a markedly different composition. There was a significant decrease (near absence) in soot, relatively high proportions of inorganic ions, and an increase in the relative proportion of NO₂ compared with NO. Concentrations of CO were also low. The low concentrations of VOCs and PM indicated that the effect of the animals on the test atmospheres was significant. The animals contributed the majority of the mass of PM in the exposure chambers through dander. They also contributed to the VOCs and to the composition of the exhaust PM through reaction of ammonia with inorganic ions and gases to form inorganic salts. The study atmospheres were employed for the successful conduct of exposure to rodents for more than 30 months (11,651 operating hours). The findings of this study will advance our understanding of the potential health benefit of the emissions reductions that have been implemented in modern diesel-powered vehicles.

ACKNOWLEDGMENTS

We would like to acknowledge the many technical staff members at LRRI and the Desert Research Institute who contributed to the successful completion of this study. In particular, Thomas Holmes, Richard White, Ramesh Chand, and Mark Gauna maintained the exposure facility, developed the exposure atmospheres, conducted the characterization, and summarized the data provided in this report. In addition, this study was enabled by the support of Craig Kazmierczak and Donald Keski-Hynnala of Daimler, the engine manufacturer representatives.

REFERENCES

- Chow JC, Watson JG, Pritchett LC, Pierson WR, Frazier CA, Purcell RG. 1993. The DRI thermal/optical reflectance carbon analysis system: description, evaluation and applications in U.S. air quality studies. *Atmos Environ*. 27A:1185–1201.
- Chow JC, Watson JG, Crow D, Lowenthal DH, Merrifield T. 2001. Comparison of IMPROVE and NIOSH carbon measurements. *Aerosol Sci Technol* 34:23–34.
- Clark N, Gautam M, Wayne W, Thompson G, Lyons D, Zhen F, et al. 2007. Creation of the heavy heavy-duty engine test schedule for representative measurement of heavy-duty engine emissions; Coordinating Research Council (CR) Report ACES-1; CRC: Alpharetta, GA; Available: <http://www.crao.org/publications/emissions/index.html>.
- Fujita EM, Zielinska B, Campbell DE, Arnott WP, Sagebiel J, Reinhart L, et al. 2007. Variations in speciated emissions from spark-ignition and compression ignition motor vehicles in the California's South Coast Air Basin. *J Air Waste Manag Assoc* 57:705–720.
- Heinrich U, Fuhst R, Rittinghausen S, Creutzenberg O, Bellmann B, Koch W, et al. 1995. Chronic inhalation exposure of Wistar rats and two different strains of mice to diesel engine exhaust, carbon black, and titanium dioxide. *Inhal Toxicol* 7:533–556.
- Khalek IA, Kittelson D, Brear F. 2000. Nanoparticle growth during dilution and cooling of diesel exhaust: experimental investigation and theoretical assessment. Society of Automotive Engineers (SAE Paper 2000-01-0515; SAE).
- Khalek IA, Bougher TL, Merritt PM. 2009. Phase 1 of the Advanced Collaborative Emissions Study. CRC Report: ACES Phase 1. Coordinating Research Council, Alpharetta GA. Available from: www.crao.org/reports/recentstudies2009/ACES%20Phase%201/ACES%20Phase1%20Final%20Report%2015JUN2009.pdf. Accessed 1/10/2011.
- Khalek IA, Bougher TL, Merritt PM, Zielinska B. 2011. Regulated and unregulated emissions from highway heavy-duty diesel engines complying with U.S. Environmental Protection Agency 2007 emissions standards. *J Air Waste Manag Assoc* 61:427–442.
- Mauderly JL, McDonald JD. 2012. Advanced Collaborative Emissions Study (ACES) Phase 3A: Characterization of U.S. 2007-Compliant Diesel Engine and Exposure System Operation. Communication 17. Health Effects Institute, Boston, MA.
- Mauderly JL, Snipes MB, Barr EB, Belinsky SA, Bond JA, Brooks AL, et al. 1994. Part I. Neoplastic and nonneoplastic lung lesions. In: *Pulmonary Toxicity of Inhaled Diesel Exhaust and Carbon Black in Chronically Exposed Rats*. Research Report 68. Health Effects Institute, Cambridge, MA.
- Mazzoleni LR, Zielinska B, Moosmüller H. 2007. Emissions of levoglucosan, methoxy phenols, and organic acids from prescribed burns, laboratory combustion of wildland fuels, and residential wood combustion. *Environ Sci Technol* 41 (7):2115–2122.
- McDonald JD, Barr EB, White RK, Chow JC, Schauer JJ, Zielinska B, et al. 2004. Generation and characterization of four dilutions of diesel engine exhaust for a subchronic inhalation study. *Environ Sci Technol* 38:2513–2522.
- McDonald JD, Doyle-Eisele M, Gigliotti A, Miller RA, Seilkop S, Mauderly JL, et al. 2012. HEI Health Review Committee. Part 1. Biologic Responses in Rats and Mice to Subchronic Inhalation of Diesel Exhaust from U.S. 2007-Compliant Engines: Report on 1-, 3-, and 12-month exposures in the ACES bioassay. *Res Rep Health Eff Inst Sep*;(166):9-120. PMID:23156840.
- Swanson J, Kittelson D, Watts W, Gladis D, Twigg M. 2009. Influence of storage and release on particle emissions from new and used CRT's. *Atmos Environ* 43:3998–4004.
- Wang Z, Fingas M, Li K. 1994a. Fractionation of a light crude oil and identification and quantification of aliphatic, aromatic, and biomarker compounds by GC-FID and GC-MS, Part I. *J Chromatograph Sci* 32:361–366.

Wang Z, Fingas M, Li K. 1994b. Fractionation of a light crude oil and identification and quantification of aliphatic, aromatic, and biomarker compounds by GC-FID and GC-MS. Part II. J Chromatograph Sci 32:367–382.

Zielinska B, Fujita EM. 2003. Characterization of ambient volatile organic compounds at the western boundary of the SCOS97-NARSTO modeling domain. Atmos Environ 37: Supplement 2, 171–180.

ADDITIONAL MATERIALS AVAILABLE ON THE WEB

Additional Materials I.A. Engine and Dilution System

Additional Materials I.B. Exposure Atmosphere Composition
Averages at High-Exposure Level During
Detailed Characterizations, and
Characterizations for April 2010, September
2010, April 2011, and April 2012

Additional Materials I.C. Exposure Summary for Routine
Monitoring of Exposure Atmospheres

Additional Materials I.D. Fuel and Oil Analyses

ABOUT THE AUTHORS

Dr. Jacob D. McDonald is the vice president for Applied Sciences as well as the director of the Environmental Respiratory Health Program at LRRRI. He has oversight of all work conducted at the LRRRI Applied Science Facility (formerly the Inhalation Toxicology Research Institute Facility). He served as principal investigator for Phase 3 of the ACES program.

Dr. Judith Chow is a research professor in the Division of Atmospheric Sciences at the Desert Research Institute. Dr. Chow oversaw the Environmental Analysis Facility that helped to support the detailed analyses performed for this research.

Dr. Barbara Zielinska is a research professor in the Division of Atmospheric Sciences at the Desert Research Institute. Dr. Zielinska oversaw the Organic Analytical Facility that helped to support the detailed analyses performed for this research.

ABBREVIATIONS AND OTHER TERMS

ACES	Advanced Collaborative Emissions Study
APS	aerosol particle sizer
CI	chemical ionization
CO	carbon monoxide
CO ₂	carbon dioxide
DE	diesel exhaust
DMM	Dekati mass monitor
DPM	diesel exhaust particulate matter
DNPH	dinitrophenylhydrazine
DPF	diesel particulate filter
EC	elemental carbon
EI	electron impact
EPA	U.S. Environmental Protection Agency
FID	flame ionization detector
FMPS	fast-mobility particle sizer
GC/MS	gas chromatography/mass spectroscopy
HCS	hydrocarbons
hr	hour
LOD	limit of detection
LRRRI	Lovelace Respiratory Research Institute
NO	nitrogen monoxide
NO ₂	nitrogen dioxide
NO _x	oxides of nitrogen
NTDE	new-technology diesel exhaust

OC	organic carbon
PAHs	polycyclic aromatic hydrocarbons
PM	particulate matter
QC	quality control
S/N	signal-to-noise ratio
SVOCs	semi-volatile organic compounds
T ₉₀	time to reach 90% of target concentration
THCs	total hydrocarbons
TOR	thermal/optical reflectance
VOCs	volatile organic compounds
XAD	polyaromatic adsorbing resins
XRF	x-ray fluorescence

Table 1. Study Engine Use By Month (Hours)*				
	2010	2011	2012	
Jan		368	<i>415</i>	
Feb	96	320	<i>362</i>	
Mar	368	368	<i>329</i>	
Apr	335 ^a	318 ^a	<i>344^a</i>	
May	353 ^b	360 ^b	<i>359^b</i>	
Jun	343	351	250	
Jul	348	348	301	
Aug	370 ^b	316	384 ^b	
Sep	344 ^{a,c}	348 ^c	403	
Oct	343	<i>381</i>	430	
Nov	351	<i>334</i>	338	
Dec	334	<i>291</i>	48 ^b	
B'	3585	3097	2154	8836
<i>B</i>		<i>1006</i>	<i>1809</i>	<i>2815</i>
			Total	11651

*Engine B values indicated by bold and italic; engine B' by regular type.

^aDates of detailed atmosphere characterizations.

^bDates of study start or animal sacrifice points.

^cDiesel particle trap replaced.

Table 2. Description of Methodology for Sampling and Analysis of Exposure Atmospheres

Analysis	Collection Device	Collection Media	Collection Point	Sample Flow Rate (L/m)	Analytical Instrument	Analytical Laboratory	Sampling Frequency ^a
gravimetric mass	aluminum in-line filter holder	Teflon filter	Chamber/ Chamber Inlet	10	MB	LRRRI	weekly
continuous mass/ black carbon	Dekati Mass Monitor/ Photoacoustic	NA	Chamber	2	NA	LRRRI	daily
Number size distribution (5–500 nm)	Fast Mobility Particle Sizer	NA	Chamber	10	FMPS	LRRRI	daily
Size distribution (0.5–20 µm)	Aerodynamic Particle Sizer	NA	Chamber	5	APS	LRRRI	detailed
nitric oxides	chemiluminescence analyzer	NA	Chamber	0.4	NA	LRRRI	daily
CO/CO ₂ /THCs	Infrared	NA	Chamber	1	NA	LRRRI	daily
organic/black carbon	aluminum in-line filter holder	quartz filter (1)	Plenum	10–50	TOR	DRI	detailed
ions (sulfate/nitrate/ ammonium)	aluminum in-line filter holder	quartz filter (2)	Plenum	10–50	IC, AC	DRI	detailed
SO ₂	UV fluorescence analyzer	NA	Chamber	1	NA	LRRRI	daily
metals and other elements	Teflon in-line filter holder	Teflon filter (2)	Plenum	20–50	ICPMS	DRI	detailed
volatile hydrocarbons (C ₁ -C ₁₂)	volatile organic sampler	electropolished canister	Chamber	0.1	GCMS/GCFID	DRI	detailed
volatile carbonyls	volatile organic sampler	DNPH cartridge	Chamber	0.3	LC/MS	DRI	detailed
semivolatile/ fine particle organics	Tisch environmental sampler	quartz filter/ XAD-4	Plenum	80	GCMS	DRI	detailed

Abbreviations: *Chemical Species*: CO = carbon monoxide; CO₂ = carbon dioxide; SO₂ = sulfur dioxide; NH₃ = ammonia; THCs = total hydrocarbons.

Instruments/Collection Devices: MB = microbalance; NA = not applicable; TOR = thermal/optical reflectance; IC = ion chromatography; ICPMS = inductively coupled plasma mass spectrometry; GCMS = gas chromatography mass spectrometry; GCFID = gas chromatography flame ionization detector; DNPH = dinitrophenylhydrazine; LC/DMS = liquid chromatography/diode array/mass spectrometry; GCMS/LCMS = gas chromatography mass spectrometry/liquid chromatography mass spectrometry; FMPS = fast mobility particle sizer; CPC = condensation particle counter; TIGF = Teflon-impregnated, glass-fiber filter; AC = automated colorimetry.

^aSampling frequency for the detailed measurements was a minimum of once/exposure level four times during the study.

Table 3A. Average^a Atmosphere Composition (\pm SD^b) During Exposure of Mice and Rats in ACES Phase 3B

Exposure Atmosphere Composition	Units	Control	Low	Mid	High
Dekati Particle Mass-Inside Chamber	$\mu\text{g}/\text{m}^3$	0.3 ± 0.2	0.2 ± 0.2	0.9 ± 0.6	6.3 ± 4
Filter Sample - Chamber Inlet	$\mu\text{g}/\text{m}^3$	NA	2.5 ± 1.6	2.7 ± 1.2	7.8 ± 2.8
Filter Sample - Inside Chamber	$\mu\text{g}/\text{m}^3$	16.9 ± 6.7	23.3 ± 11.4	20 ± 5.4	27.3 ± 6.2
Particle Mass - FMPS ^c	$\mu\text{g}/\text{m}^3$	0.2 ± 0.2	1.1 ± 0.9	2 ± 1.7	5.3 ± 2.9
Particle Count - FMPS ^c	Particle/cm ³	17136 ± 23420.5	215225.5 ± 412548.9	678184 ± 1247908.6	828814.3 ± 1041924.8
NMAD ^{a,b} - FMPS ^c	nm	$23 (1.8) \pm 8.8 (0.5)$	$16.6 (1.5) \pm 6.3 (0.2)$	$15.4 (1.5) \pm 5.5 (0.2)$	$18.6 (1.6) \pm 4.4 (0.1)$
MMAD ^{a,b} - FMPS ^c	nm	$196.8 (1.7) \pm 149 (0.2)$	$181.8 (2.7) \pm 113.4 (0.6)$	$81.2 (2.9) \pm 32 (0.8)$	$41.6 (2.2) \pm 4.1 (0.5)$
Nitrogen Oxide (NO)	$\mu\text{g}/\text{m}^3$ (ppm)	$2 \pm 3 (0.001 \pm 0.002)$	$274.3 \pm 186.3 (0.3 \pm 0.2)$	$1376.6 \pm 390.4 (1.3 \pm 0.4)$	$6878.6 \pm 2591.8 (6.6 \pm 2.4)$
Nitrogen Dioxide (NO ₂)	$\mu\text{g}/\text{m}^3$ (ppm)	$2.6 \pm 5.2 (0.002 \pm 0.004)$	$159.5 \pm 16.6 (0.1 \pm 0.01)$	$1421.5 \pm 83.7 (0.9 \pm 0.05)$	$6873.2 \pm 489.4 (4.4 \pm 0.3)$
Carbon Monoxide (CO) ^c	$\mu\text{g}/\text{m}^3$ (ppm)	$895.8 \pm 883.2 (0.9 \pm 0.9)$	$1042.2 \pm 510.1 (1.1 \pm 0.5)$	$1787.1 \pm 444 (1.9 \pm 0.5)$	$6167.6 \pm 2445.4 (6.4 \pm 2.6)$
Carbon Dioxide (CO ₂) ^c	mg/m ³ (ppm)	2110.6 ± 800.1 (1402.2 ± 531.7)	2695.7 ± 1175.2 (1790.9 ± 780.9)	3599.1 ± 497.8 (2391.2 ± 330.8)	7215.6 ± 1456.4 (4794.1 ± 967.5)
Sulfur Dioxide (SO ₂)	$\mu\text{g}/\text{m}^3$ (ppb)	$4.9 \pm 1 (2.2 \pm 0.4)$	$6.6 \pm 1.5 (2.9 \pm 0.7)$	$20.5 \pm 6.2 (9.1 \pm 2.7)$	$69.6 \pm 28.6 (30.8 \pm 12.6)$
Elemental Carbon ^c	$\mu\text{g}/\text{m}^3$	0.4 ± 0.4	1.2 ± 1.2	0.4 ± 0.4	1.2 ± 1
Organic Carbon ^c	$\mu\text{g}/\text{m}^3$	4.5 ± 1.4	6.6 ± 1.4	4.8 ± 1.9	5.7 ± 2.4
Ammonium ^c	ng/m ³	31.3 ± 31.3	57.2 ± 29	203.2 ± 150.6	1312.2 ± 450.2
Sulfate ^c	ng/m ³	101.6 ± 26	193.1 ± 153.1	644.8 ± 405.5	2121.1 ± 968.2
Nitrate ^c	ng/m ³	18.6 ± 16.7	181.2 ± 195.9	220.2 ± 73.9	2087.3 ± 747
Elements (Metals) ^c	ng/m ³	461.3 ± 208.5	567.9 ± 224	661 ± 302.1	811.5 ± 336.3
Alkanes ^c	$\mu\text{g}/\text{m}^3$	2.8 ± 0.5	4.7 ± 1.9	8.6 ± 2.8	26.6 ± 9.3
Carbonyl ^c	$\mu\text{g}/\text{m}^3$	53.8 ± 12.1	71.2 ± 40.2	21.4 ± 5.1	1 ± 1.5
Polycyclic Aromatic Hydrocarbon (PAH) ^c	$\mu\text{g}/\text{m}^3$	0.8 ± 0.5	1.1 ± 0.4	1.9 ± 0.7	4.7 ± 1.6
Nitro-PAH	ng/m ³	0.4 ± 0.2	0.8 ± 0.4	1.6 ± 0.5	8 ± 2.5
Polars (Acids) ^c	$\mu\text{g}/\text{m}^3$	3.2 ± 1.2	4.1 ± 1.6	6.9 ± 2.9	16 ± 6
Hopane and Steranes ^c	ng/m ³	2 ± 0.7	5.1 ± 3.5	2.5 ± 1.6	3.7 ± 3.9
Volatile Organic Compounds (VOCs) ^c	$\mu\text{g}/\text{m}^3$	33.5 ± 21.3	50.3 ± 31.3	44.2 ± 15.3	148.9 ± 96.9

Abbreviations: FMPS = fast mobility particle sizer; MMAD = mass median aerodynamic diameter; NA = not available (no data were collected during that period due to study design); NMAD = number median aerodynamic diameter.

^aAverage concentrations for each analyte are averages of all available measurements throughout the study for each analyte.

^b Or geometric standard deviation where indicated.

^c Derived from detailed characterizations (April 2010 [engine B¹], September 2010 [engine B¹], April 2011 [engine B¹], April 2012 [engine B]). (See Additional Materials I.B.)

Table 3B. Daily Average^a Atmosphere Composition \pm (SD^b) During Exposure of Rats During ACES Phase 3B

Exposure Atmosphere Composition	Units	Control	Low	Mid	High
Dekati Particle Mass-Inside Chamber	$\mu\text{g}/\text{m}^3$	0.4 ± 0	0.3 ± 0.2	1.07 ± 0.7	12.3 ± 13.6
Filter Sample - Chamber Inlet	$\mu\text{g}/\text{m}^3$	NA	3.3 ± 5.4	5.1 ± 4.4	11.9 ± 6.3
Filter Sample - Inside Chamber	$\mu\text{g}/\text{m}^3$	26.6 ± 16.4	24.9 ± 15.6	30.4 ± 19.2	30.5 ± 15.6
Particle Mass - FMPS ^c	$\mu\text{g}/\text{m}^3$	0.2 ± 0.2	1.1 ± 0.9	2 ± 1.7	5.3 ± 2.9
Particle Count - FMPS ^c	Particle/cm ³	17136 ± 23420.5	215225.5 ± 412548.9	678184 ± 1247908.6	828814.3 ± 1041924.8
NMAD ^b - FMPS ^c	nm	$23 (1.8) \pm 8.8 (0.5)$	$16.6 (1.5) \pm 6.3 (0.2)$	$15.4 (1.5) \pm 5.5 (0.2)$	$18.6 (1.6) \pm 4.4 (0.1)$
MMAD ^b - FMPS ^c	nm	$196.8 (1.7) \pm 149 (0.2)$	$181.8 (2.7) \pm 113.4 (0.6)$	$81.2 (2.9) \pm 32 (0.8)$	$41.6 (2.2) \pm 4.1 (0.5)$
NO	$\mu\text{g}/\text{m}^3$ (ppm)	$1.1 \pm 3.6 (0.001 \pm 0.004)$	$449.4 \pm 285.5 (0.4 \pm 0.3)$	$1722.0 \pm 422.8 (1.7 \pm 0.4)$	$7733.5 \pm 1933.4 (7.5 \pm 1.9)$
NO ₂	$\mu\text{g}/\text{m}^3$ (ppm)	$0.0 \pm 18.8 (0.0 \pm 0.012)$	$164.6 \pm 23.3 (0.1 \pm 0.02)$	$1378.4 \pm 158.9 (0.9 \pm 0.10)$	$6654.4 \pm 597.9 (4.2 \pm 0.4)$
CO	$\mu\text{g}/\text{m}^3$ (ppm)	NA	NA	NA	$5737.2 \pm 2595.6 (6.0 \pm 2.7)$
CO ₂	mg/m^3 (ppm)	NA	NA	NA	$7697.1 \pm 704.4 (5113.8 \pm 468.4)$
SO ₂	$\mu\text{g}/\text{m}^3$ (ppb)	NA	NA	NA	$70.1 \pm 20.9 (31.1 \pm 9.3)$

Abbreviations: CO₂ = carbon dioxide; CO = carbon monoxide; DMM = Dekati mass monitor; FMPS = fast-mobility particle sizer; MMAD = mass median aerodynamic diameter; NA = not available (no data were collected during that period due to study design); NMAD = number median aerodynamic diameter; NO = nitrogen monoxide; NO₂ = nitrogen dioxide; SO₂ = sulfur dioxide.

^aFor each day indicated, the average is an integrated average of all measurements obtained throughout the day. In some cases only one measurement could be obtained per day but in others (i.e., gas data) the values were obtained at higher frequencies.

^b Or geometric standard deviation where indicated.

^c FMPS data collected during detailed characterizations, not entire study.

Table 4. Temporal Comparison of Average^a (\pm SD^b) for the High-Level Exposure Atmosphere Composition During the Detailed Characterizations

	Units	April 2010	September 2010	April 2011	April 2012
		(engine B', mice)	(engine B', rat)	(engine B', rat)	(engine B, rat)
		High	High	High	High
Dekati Particle Mass - Chamber Inlet	$\mu\text{g}/\text{m}^3$	NA	NA	NA	NA
Dekati Particle Mass - Inside Chamber	$\mu\text{g}/\text{m}^3$	10.3 \pm 5.2	9.04 \pm 11.8	2 \pm 0.8	3.8 \pm 2.8
Filter Sample - Chamber Inlet	$\mu\text{g}/\text{m}^3$	8.3 \pm 2.1	8.0 \pm 3.0	4 \pm 1	10.7 \pm 0.5
Filter Sample - Inside Chamber	$\mu\text{g}/\text{m}^3$	28.3 \pm 23.0	20.0 \pm 2.0	35 \pm 44	26.0 \pm 9.3
Particle Mass - FMPS	$\mu\text{g}/\text{m}^3$	2.93 \pm 0.84	6.23 \pm 3.89	3.1 \pm 1.4	9.12 \pm 0.47
Particle Count - FMPS	Particle/cm ³	9.68e+04 \pm 1.66e+04	2.37E06 \pm 1.16E+06	5.2E05 \pm 1.6E+05	328457 \pm 121864
NMAD ^b - FMPS	nm	20.17 (1.55) \pm 6.40 (0.05)	12.1 (1.7) \pm 0.5 (0.1)	14.5 (1.5) \pm 1.0 (0.03)	21.1 (1.6) \pm 2.1 (0.02)
MMAD ^b - FMPS	nm	44.17 (2.53) \pm 1.72 (0.71)	35.5 (1.8) \pm 3.1 (0.1)	29.6 (1.8) \pm 3.7 (0.2)	43.3 (2.8) \pm 2.0 (0.4)
Nitrogen Oxide (NO)	$\mu\text{g}/\text{m}^3$ (ppm)	4875 \pm 728 (4.75 \pm 0.71)	4936.1 \pm 738.9 (4.8 \pm 0.7)	7338.5 \pm 142.1 (7.2 \pm 0.1)	10364.7 \pm 1949.8 (9.8 \pm 1.9)
Nitrogen Dioxide (NO ₂)	$\mu\text{g}/\text{m}^3$ (ppm)	6389 \pm 1448 (4.06 \pm 0.92)	6813.3 \pm 1148.7 (4.3 \pm 0.7)	6737.5 \pm 204.0 (4.3 \pm 0.1)	7552.9 \pm 1416.2 (4.8 \pm 0.9)
Carbon Monoxide (CO)	$\mu\text{g}/\text{m}^3$ (ppm)	5977 \pm 785 (6.24 \pm 0.82)	9453.4 \pm 1724.0 (9.9 \pm 1.8)	5696.3 \pm 518.9 (5.9 \pm 0.5)	3543.8 \pm 383.1 (3.7 \pm 0.4)
Carbon Dioxide (CO ₂)	mg/m ³ (ppm)	5388 \pm 343 (3580 \pm 228)	8950.9 \pm 681.9 (5947.0 \pm 453.1)	7322.3 \pm 59.1 (4865 \pm 39.3)	7201.0 \pm 185.0 (4784.4 \pm 122.9)
Sulfur Dioxide (SO ₂)	$\mu\text{g}/\text{m}^3$ (ppb)	53.2 \pm 9 (23.6 \pm 3.88)	43.8 \pm 11.7 (19.4 \pm 5.2)	73.0 \pm 2.2 (32.3 \pm 1.0)	108.4 \pm 3.61 (48 \pm 1.6)
Elemental Carbon	$\mu\text{g}/\text{m}^3$	2.7 \pm 0.15	1.0	0.7 \pm 0.02	0.4 \pm 0.1
Organic Carbon	$\mu\text{g}/\text{m}^3$	6.1 \pm 0.20	2.6 \pm 0.04	5.5 \pm 0.3	8.5 \pm 0.4
Ammonium	ng/m ³	1740.4 \pm 0.3	1374.3 \pm 27.3	679.4 \pm 112.4	1454.8 \pm 5.4
Sulfate	ng/m ³	1740.4 \pm 0.9	2863.7 \pm 4.0	927.5 \pm 0.1	2952.6 \pm 3.8
Nitrate	ng/m ³	1193.3 \pm 0.4	2975 \pm 0.5	2298.4 \pm 1.9	1882.3 \pm 50.9
Elements (Metals)	ng/m ³	823.8 \pm 240.8	712.0 \pm 226.2	451.7 \pm 6.7	1258.5 \pm 29.2
Alkanes	ng/m ³	26.7 \pm 1.5	16 \pm 0.9	24.9 \pm 1.3	38.6 \pm 2
Carbonyl	$\mu\text{g}/\text{m}^3$	0.3 \pm 1.0	3.3 \pm 0.5	0.4 \pm 0.4	0 \pm 0.3
Polycyclic Aromatic Hydrocarbons (PAHs)	$\mu\text{g}/\text{m}^3$	6.2 \pm 0.3	3.8 \pm 0.3	6 \pm 0.33	2.89 \pm 0.18
Nitro-PAHs	ng/m ³	6.5 \pm 0.4	5.5 \pm 0.3	8.6 \pm 0.46	11.2 \pm 1
Polars (Acids)	ng/m ³	24.8 \pm 2.2	12.1 \pm 1	15 \pm 0.8	12.1 \pm 1
Hopane and Steranes	ng/m ³	0.9 \pm 0.1	1.3 \pm 0.2	3.1 \pm 0.2	9.3 \pm 0.7
Volatile Organic Compounds (VOCs)	$\mu\text{g}/\text{m}^3$	74.9 \pm 12.8	73.6 \pm 10	169.1 \pm 17.3	277.8 \pm 16.3

Abbreviations: FMPS = fast-mobility particle sizer; MMAD = mass median aerodynamic diameter; NA = not applicable; NMAD = number median aerodynamic diameter.

^a For each day indicated, the average is an integrated average of all measurements obtained throughout the day.

^b Or geometric standard deviation where indicated.

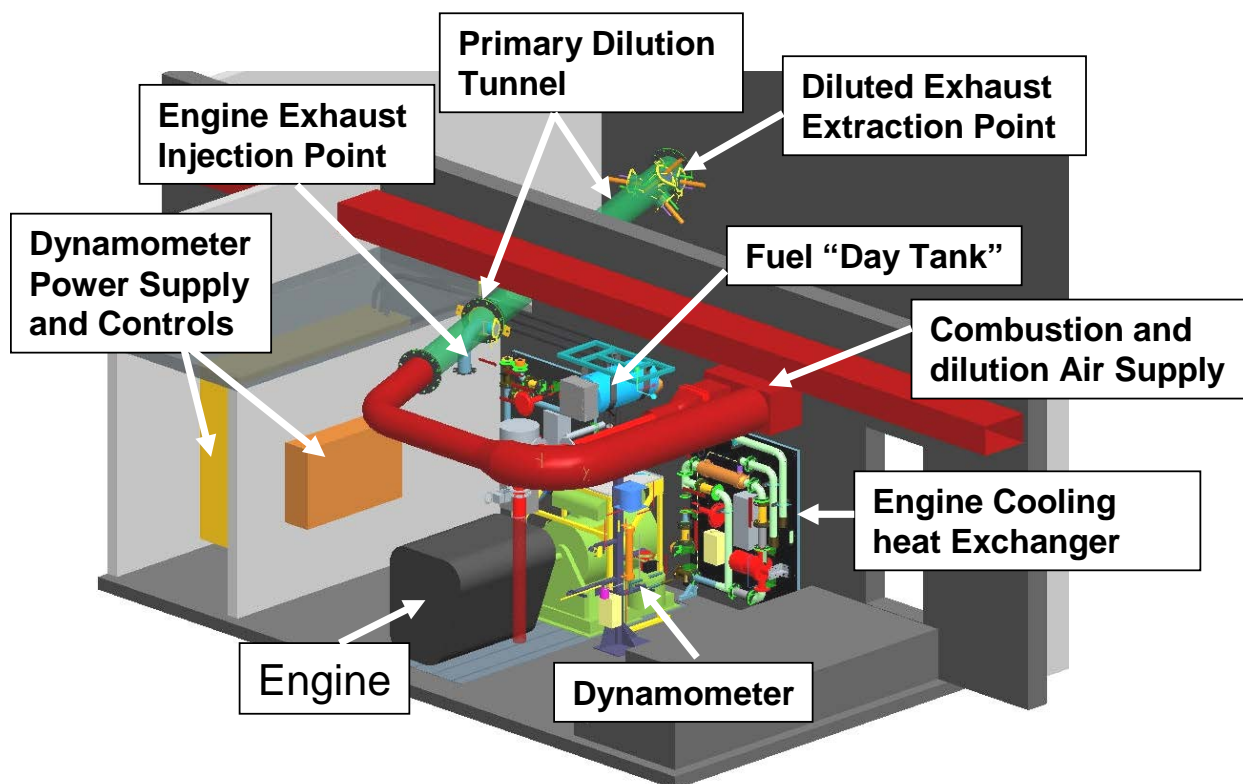


Figure 1. Front quarter view of engine laboratory and dilution tunnel. The tunnel portions shown in red are prior to mixing of the engine exhaust. The green area shows the exhaust mixing section and the take-off point for the exposure chamber distribution system. The engine is shown in black, and the fuel delivery system in blue. The dynamometer is shown in light green. The DPF is not shown. It was placed in between the engine and the engine exhaust injection point.

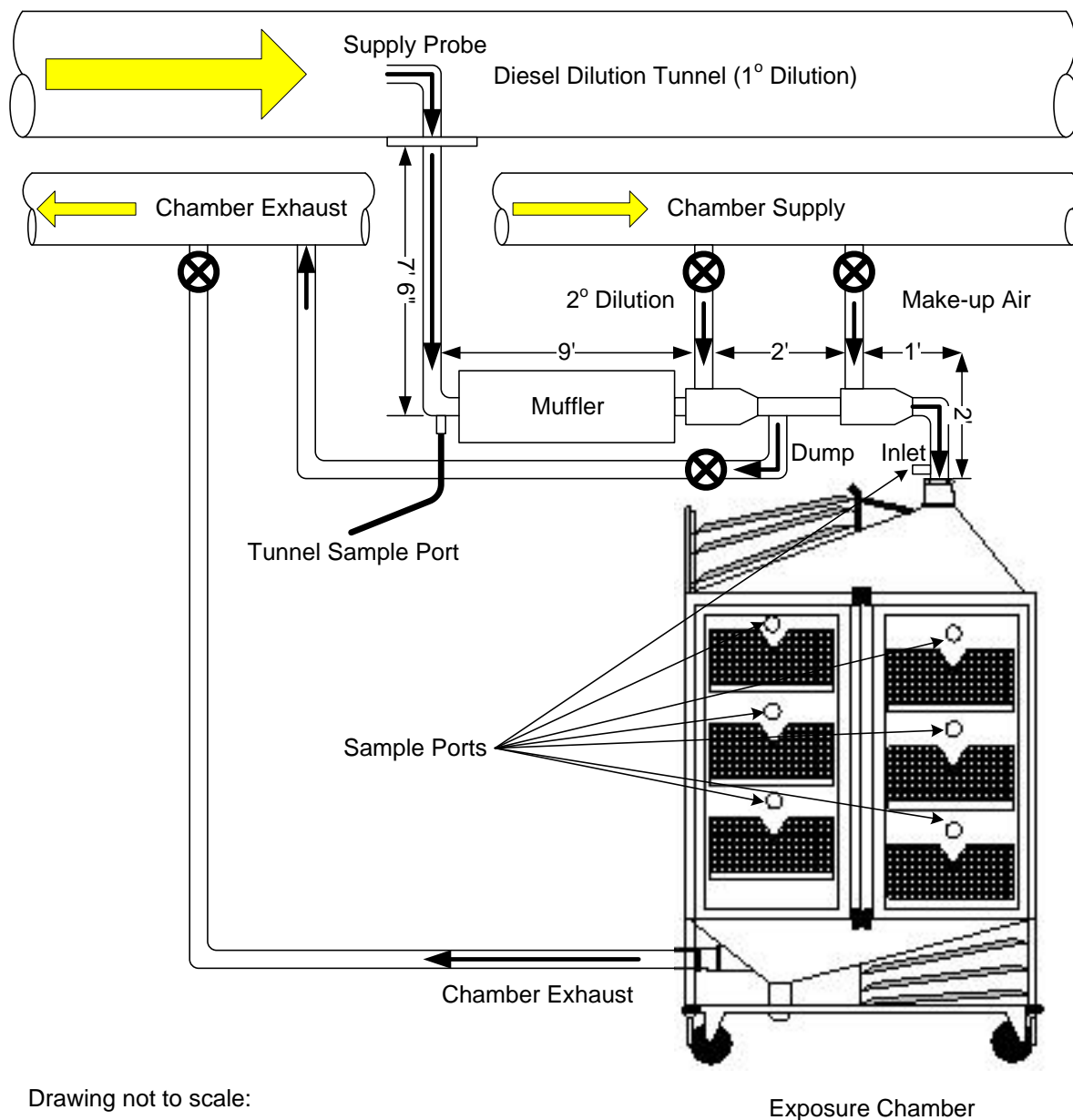


Figure 2. Schematic (not to scale) of secondary (2°) and tertiary (make-up air) dilution system prior to inhalation exposure chamber. Diluted exhaust is extracted through a sampling probe. The probe size scales from 0.95–5 cm, with the smallest size extraction for the lowest exposure level and the largest for the highest level. Flows to the chambers were extracted by house vacuum. Aerosols were carried through a flow-through muffler prior to a series of two bypass and dilution legs.

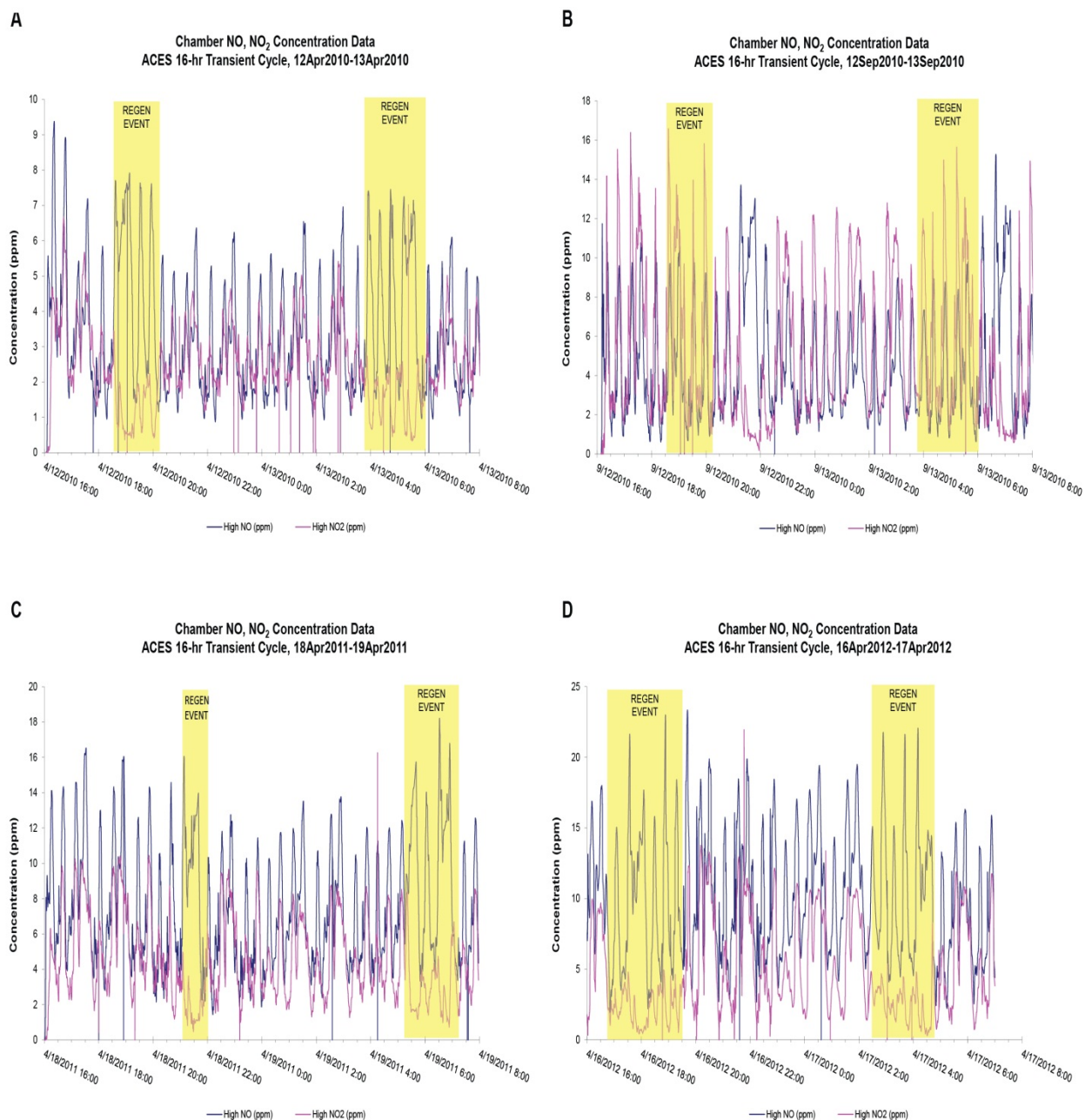


Figure 3. Representative real-time concentrations of NO and NO₂ during a 16-hr ACES transient cycle on four different days. Data were obtained from the high-exposure level (4.2 ppm average NO₂ target) during parallel “detailed” measurements of test atmospheres made in April 2010 (Panel A, engine B’, mice), September 2010 (Panel B, engine B’, rats), April 2011 (Panel C, engine B’, rats), and April 2012 (Panel D, engine B, rats).

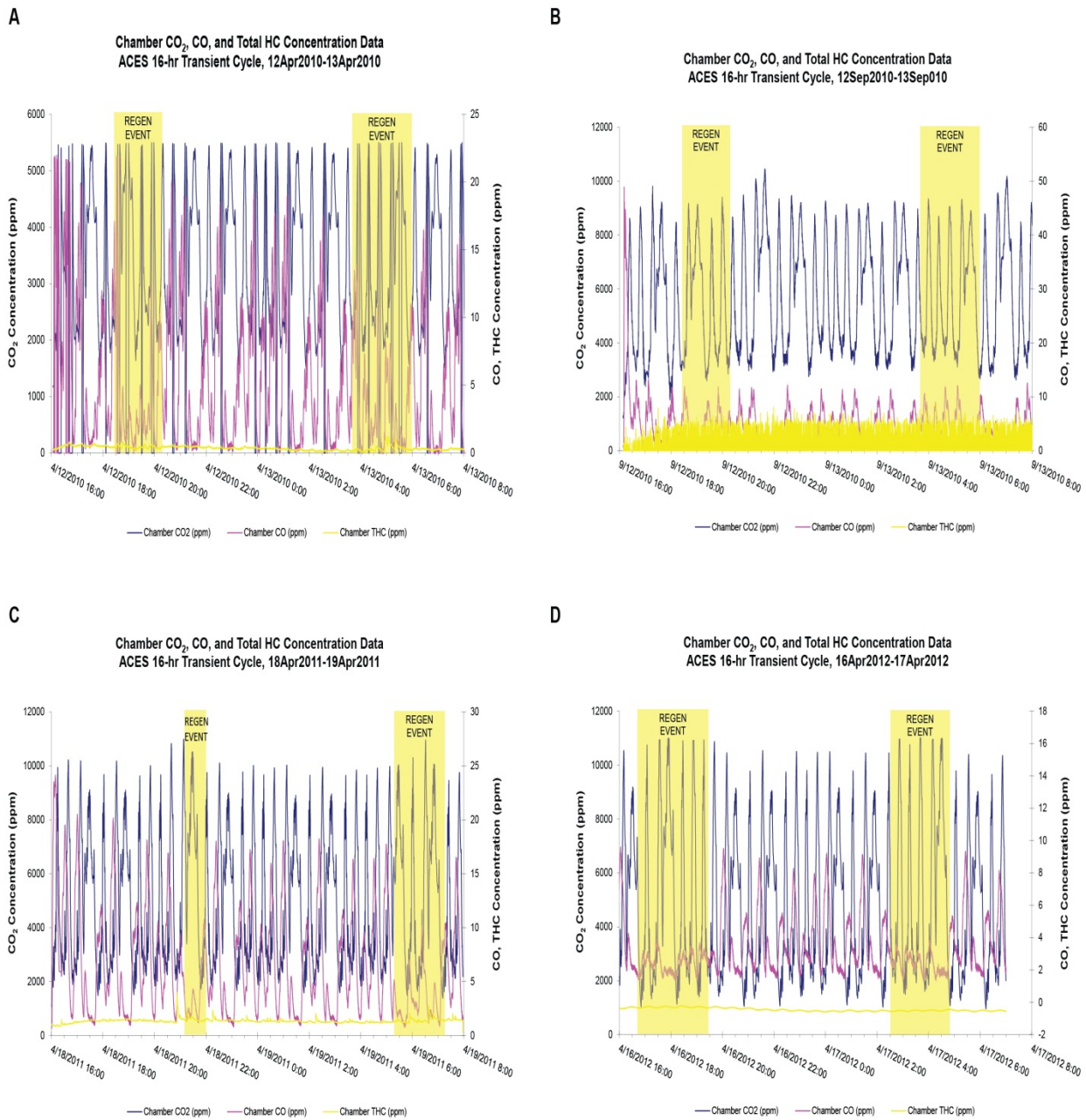


Figure 4. Representative real-time concentrations of CO₂, CO, and HC (indicated as THC) during a 16-hr ACES transient cycle. Data were obtained from high-exposure level measurements made in April 2010 (Panel A, engine B', mice), September 2010 (Panel B, engine B', rats), April 2011 (Panel C, engine B', rats), and April 2012 (Panel D, engine B, rats).

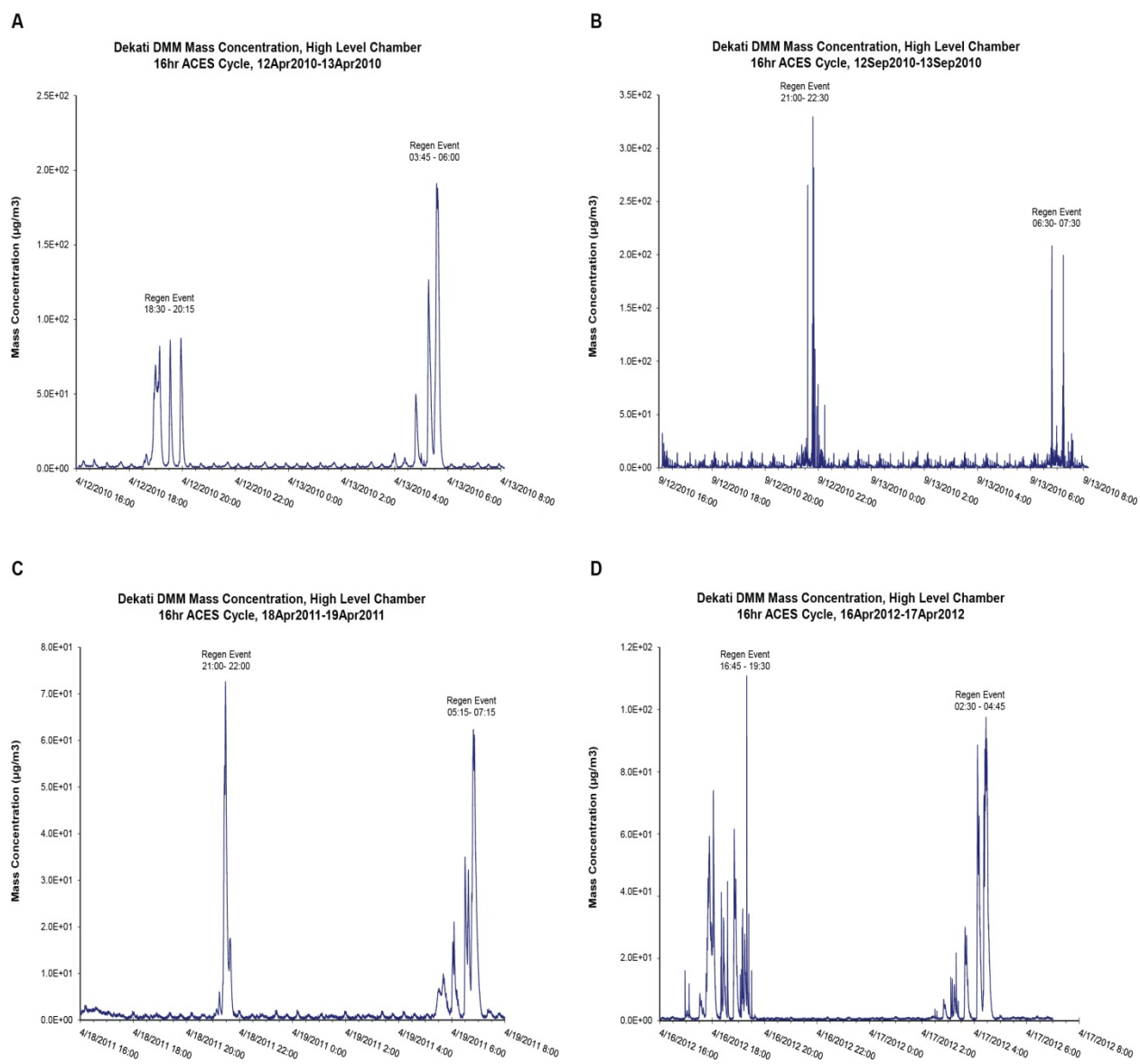
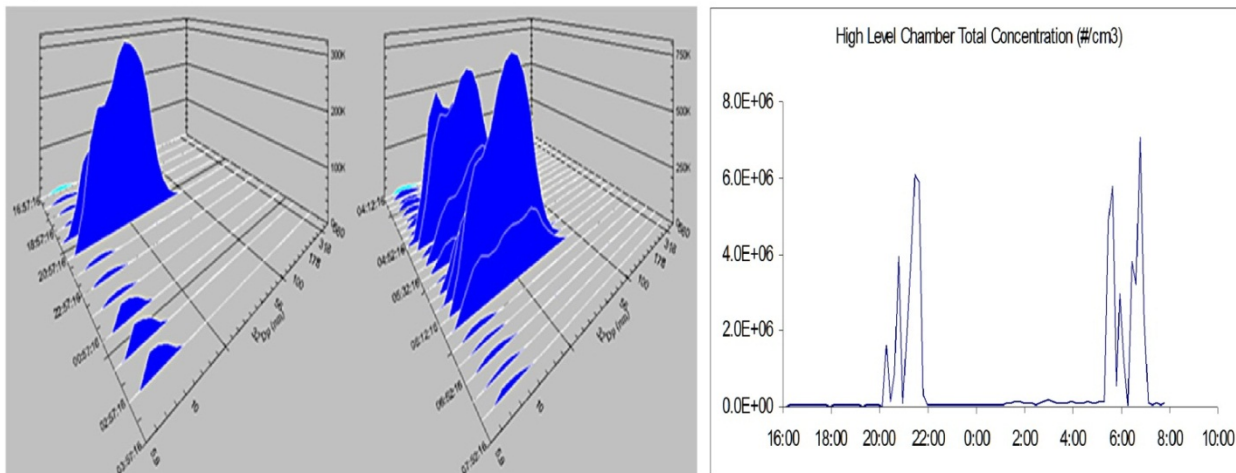


Figure 5. Representative real-time particle mass concentrations measured by the DMM. Particle concentrations peaked during the DPF regenerations. Data are from measurements made in April 2010 (Panel A, engine B', mice), September 2010 (Panel B, engine B', rats), April 2011 (Panel C, engine B', rats), and April 2012 (Panel D, engine B, rats).

September 2010



April 2012

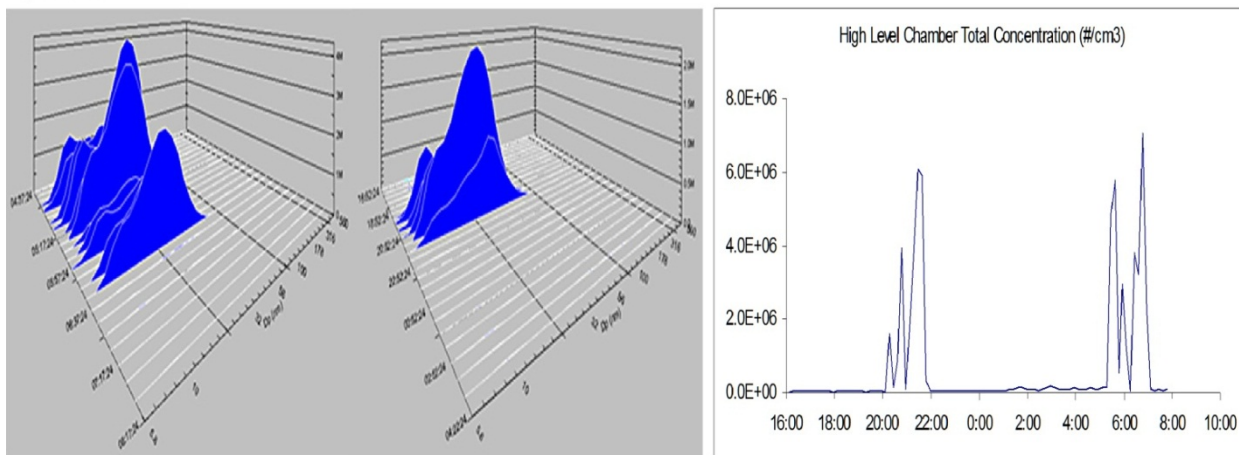


Figure 6. Representative real-time particle size and number concentrations measured by the FMPS. Particle concentrations peaked during the DPF regenerations. Data are measurements made in September 2010 (top right panel, engine B', rats) and April 2012 (bottom right panel, engine B, rats).

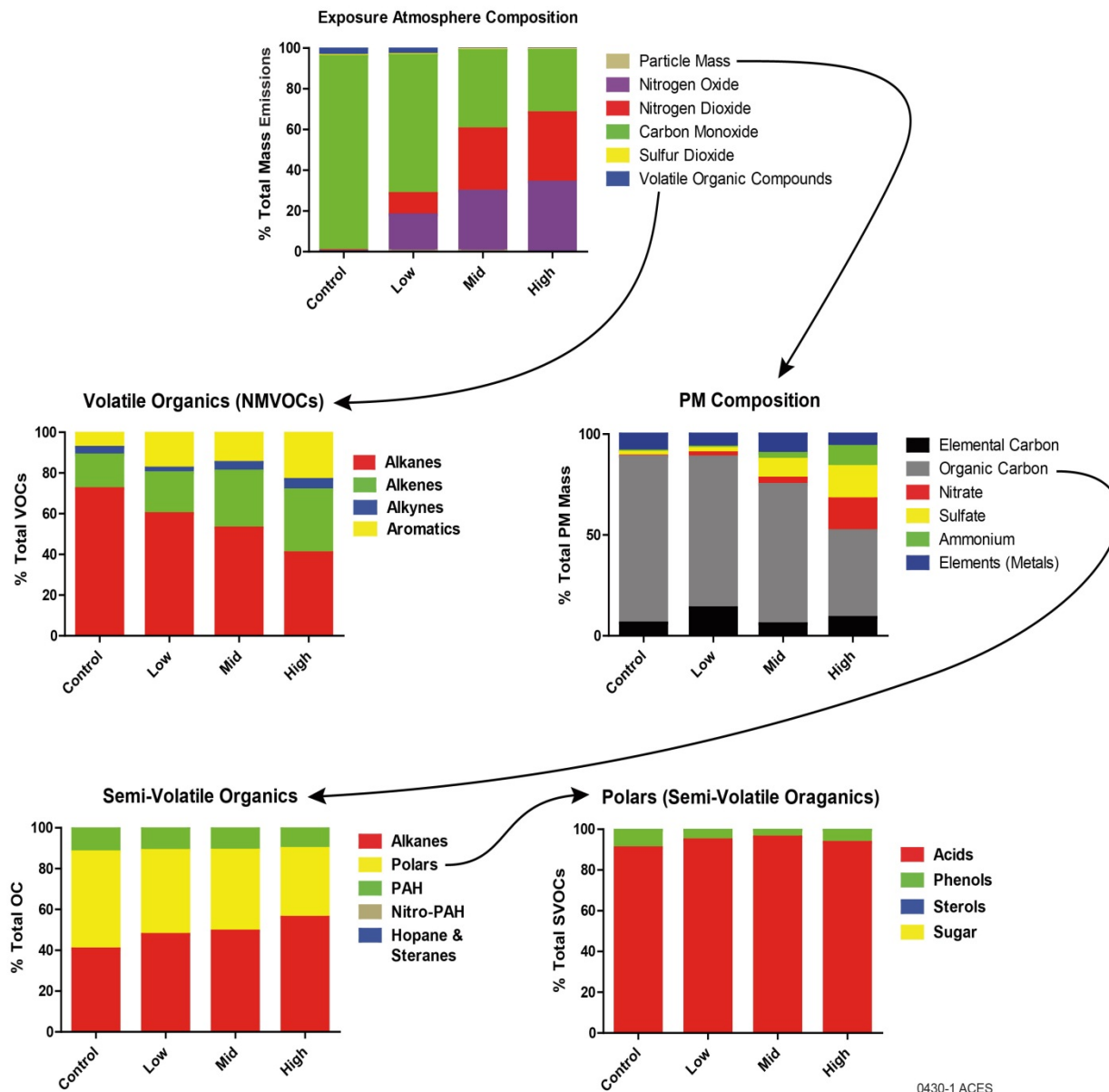


Figure 7. Average exposure atmosphere composition during the ACES chronic bioassay. Percent contributions for each chemical class are shown. Data are averages of measurements made in April 2010 (engine B', mice), September 2010 (engine B', rats), April 2011 (engine B', rats), and April 2012 (engine B, rats).

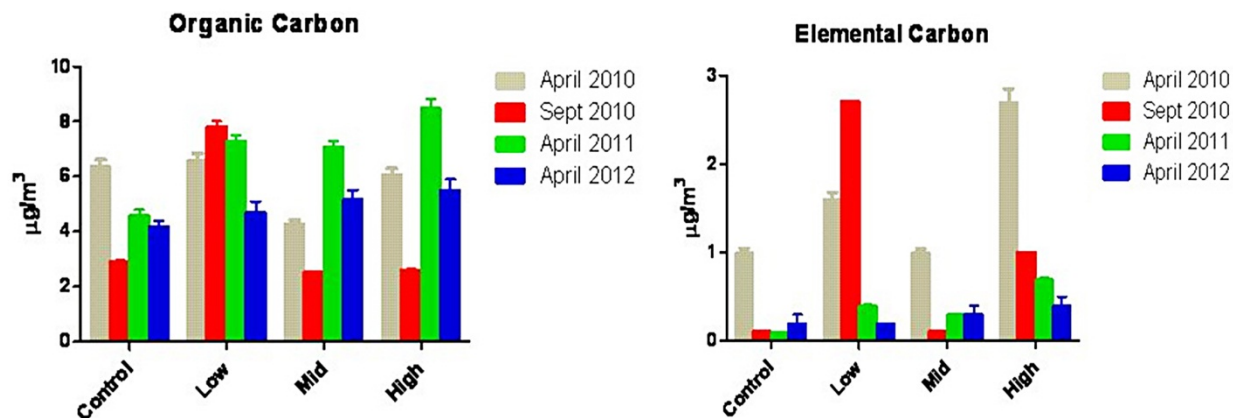


Figure 8. Concentrations of organic carbon and elemental carbon at each exposure level in April 2010 (engine B', mice), September 2010 (engine B', rats), April 2011 (engine B', rats), and April 2012 (engine B, rats).

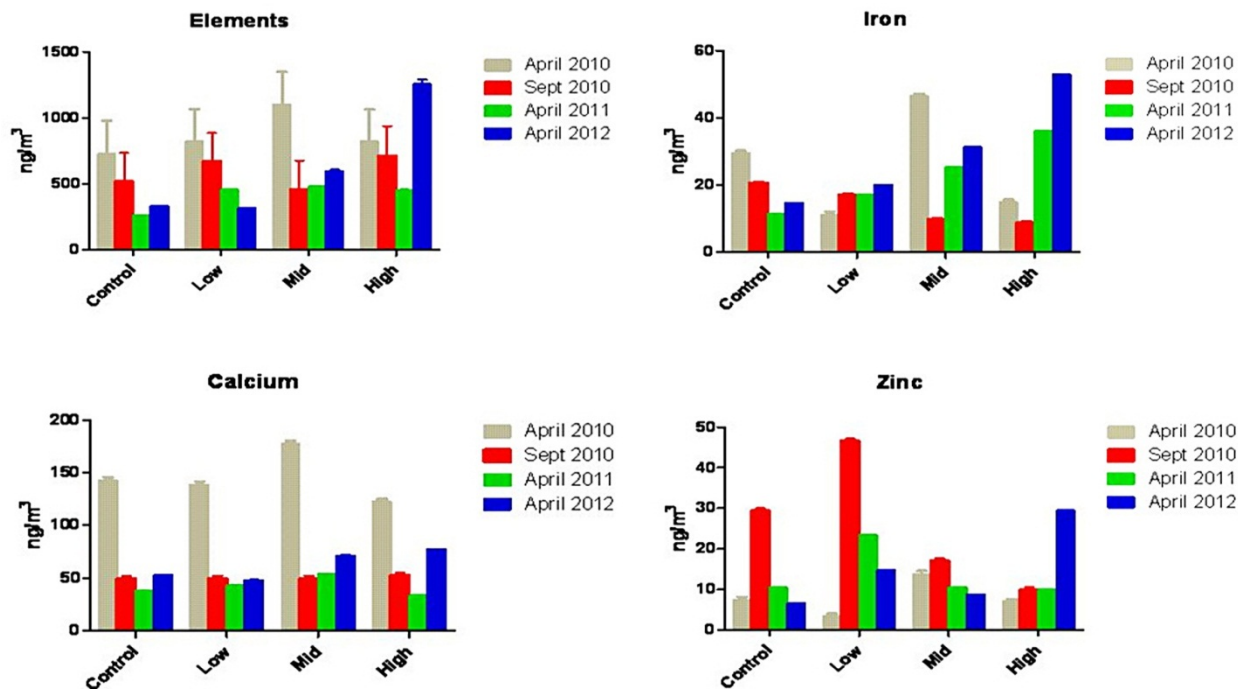


Figure 9. Concentrations of total sum of elements, as well as iron, calcium, and zinc in April 2010 (engine B', mice), September 2010 (engine B', rats), April 2011 (engine B', rats), and April 2012 (engine B, rats).

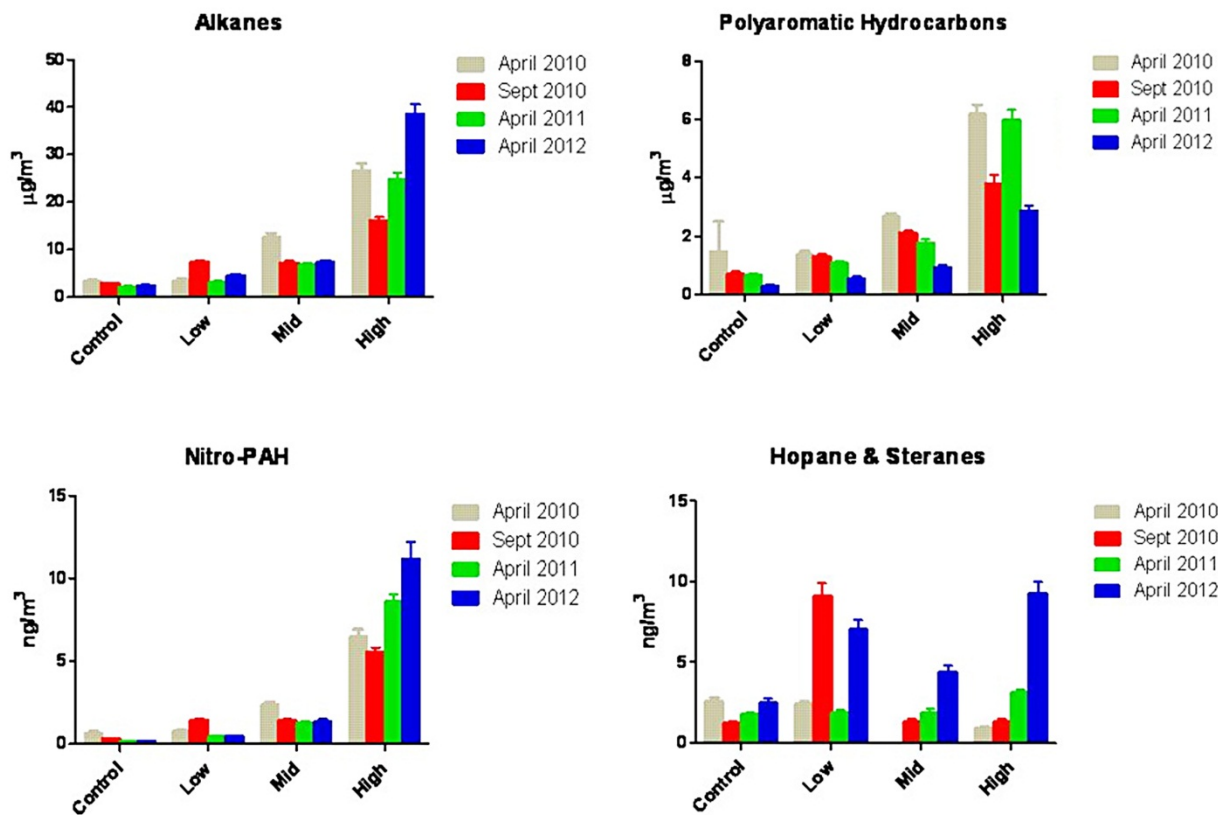


Figure 10. Concentrations of semivolatile alkanes, PAHs, nitro-PAHs, and hopanes/steranes in April 2010 (engine B', mice), September 2010 (engine B', rats), April 2011 (engine B', rats), and April 2012 (engine B, rats).